



Oxygen isotope ecology of recent planktic foraminifera at the central Walvis Ridge (SE Atlantic)

Neven Lončarić,¹ Frank J. C. Peeters,² Dick Kroon,^{2,3} and Geert-Jan A. Brummer¹

Received 26 August 2005; revised 4 February 2006; accepted 14 April 2006; published 16 August 2006.

[1] Above the Walvis Ridge, in the SE Atlantic Ocean, we collected living planktic foraminifera from the upper water column using depth stratified plankton tows. The oxygen isotope composition ($\delta^{18}\text{O}_c$) in shells of foraminifera and shell concentration profiles show seasonal and depth habitats of individual species. The tow results are compared with the average annual deposition $\delta^{18}\text{O}_c$ from sediment traps and the interannual average $\delta^{18}\text{O}_c$ of fossil specimens in top sediments at the same site. The species *Globigerinita glutinata* best reflects the austral winter/spring sea surface temperature (SST). Its $\delta^{18}\text{O}_c$ signal in top sediments remains pristine. In contrast, tow results also show that *Globigerinoides ruber* continues to calcify below the surface mixed layer (SML), i.e., down to the deep chlorophyll maximum (DCM); hence its $\delta^{18}\text{O}_c$ signature of exported specimens reflects the SST only when SML incorporates the DCM. Deep tow and sediment trap results show that both *Globorotalia truncatulinoides* and *Globorotalia inflata* record the temperature between 150 and 350 m, depending on the season and the shell size. However, for all fossil taxa in sediments apart from *Globigerinita glutinata*, we observe a positive $\delta^{18}\text{O}_c$ shift with respect to the sediment trap and plankton tow values, likely related to the interannual flux changes and deep encrustation.

Citation: Lončarić, N., F. J. C. Peeters, D. Kroon, and G.-J. A. Brummer (2006), Oxygen isotope ecology of recent planktic foraminifera at the central Walvis Ridge (SE Atlantic), *Paleoceanography*, 21, PA3009, doi:10.1029/2005PA001207.

1. Introduction

[2] Stable oxygen isotope composition ($\delta^{18}\text{O}$) of the foraminiferal carbonate shell has been used widely for estimates of past global ice volume/sea level [e.g., *Shackleton and Opdyke*, 1973], sea surface temperature [e.g., *Erez and Luz*, 1983; *Deuser*, 1987], salinity [e.g., *Duplessy et al.*, 1992] and ocean stratification [*Williams et al.*, 1981; *Mulitza et al.*, 1997; *Niebler et al.*, 1999; *Simstich et al.*, 2003]. Yet, the seawater temperature derived from foraminiferal $\delta^{18}\text{O}$ can only be quantified and understood from sediment cores when the foraminiferal depth habitat and seasonal distribution are known. Field observations on living foraminifera are therefore necessary, allowing direct comparison of $\delta^{18}\text{O}$ in shells with the physical and chemical properties of the ambient water column. In this way foraminiferal depth habitat and isotopic disequilibrium (i.e., the offset from a given temperature equation) can be quantified [*Fairbanks et al.*, 1980, 1982; *Ortiz et al.*, 1996; *Peeters and Brummer*, 2002; *Mulitza et al.*, 2003a], essential to constrain paleotemperature estimates and arrive at more robust reconstructions of past hydrographic conditions.

[3] In this paper we present results on an integrated study on ecology of planktic foraminifera and their associated

isotope signal from the central Walvis Ridge (CWR) site, in the South Atlantic Ocean. In order to unravel the process from shell production to sediment preservation, we discuss the seasonal and vertical distribution, ecology and oxygen isotope composition of a number of species from plankton tows, sediment traps and a box corer. The shell concentration profiles of species *Globigerinoides trilobus*, *Globigerinoides ruber*, *Globigerinita glutinata*, *Globorotalia truncatulinoides*, and *Globorotalia inflata* and the oxygen isotope composition of their shells are examined to estimate the calcification temperature for exported specimens, thereby providing direct information on the depth habitat in contrasting seasons. We quantify the oxygen isotope offset from equilibrium within the productive zone in the upper water column (i.e., the interval where foraminifer calcifies its shell) and determine the isotopic signature of the exported shells at greater depth. Since the flux of planktic foraminifera is seasonally variable [e.g., *Deuser et al.*, 1981; *Thunell and Sautter*, 1992; *Schiebel and Hemleben*, 2000], we also compare the annual flux-weighted $\delta^{18}\text{O}$ of different species from the sediment traps to the $\delta^{18}\text{O}$ of fossil specimens on the seafloor directly underneath. Our goal was to examine which species is the best proxy of the sea surface temperature (SST), how this water column signal gets transferred to the seafloor, and to which extent it gets preserved in the top sediments.

2. Material

2.1. Plankton Tows

[4] During the Mixing of *Agulhas* Rings Experiment (MARE) cruises in February 2000, July 2000, and February

¹Department of Marine Chemistry and Geology, Royal Netherlands Institute for Sea Research, Den Burg, Texel, Netherlands.

²Department of Paleocology and Paleoclimatology, Faculty of Life and Earth Sciences, Vrije Universiteit Amsterdam, Amsterdam, Netherlands.

³Now at Department of Geology and Geophysics, University of Edinburgh, Edinburgh, UK.

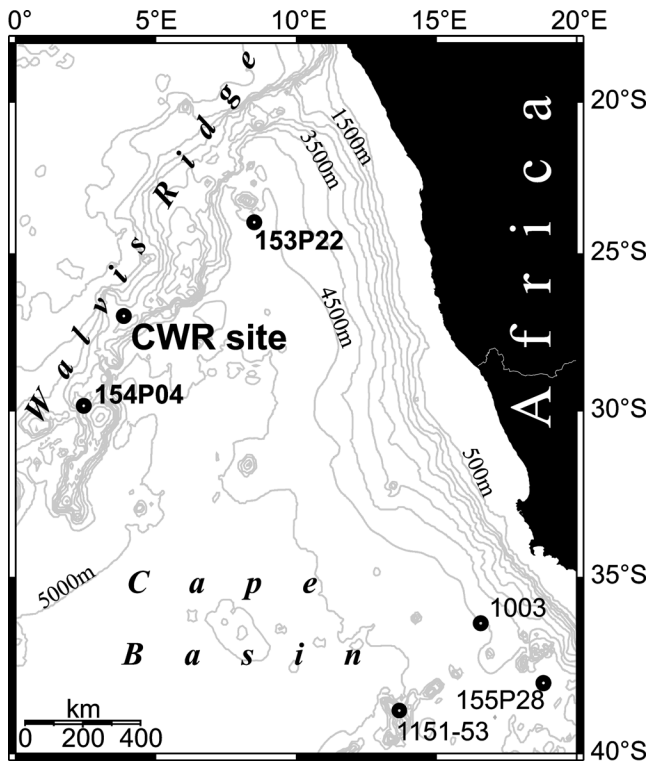


Figure 1. Regional bathymetry and location of the CWR site sampled by CTD, plankton tows, sediment traps, and box corer. The water samples used for the $\delta^{18}\text{O}_w$ measurements (Figure 3) were taken at three Walvis Ridge sites. Additional $\delta^{18}\text{O}_c$ data for *G. glutinata* (Figure 8) is from the southern Cape Basin.

2001, depth stratified plankton tows were collected at the CWR site (Figure 1 and Table 1). Each station covered nine depth intervals from the upper 800–1000 m of the water column. The plankton was collected using a Hydrobios multinet system modified for oblique towing and equipped with two flowmeters and five plankton nets with a 100 μm mesh (Table 1). The nets were successively opened and closed during the upcast while obliquely towed behind the ship, sampling approximately 130–1000 m^3 of seawater for the deep cast and 20–180 m^3 for the shallow cast (Table 1) (for further details on plankton sampling equipment, see *Wiebe and Benfield* [2003]). Large metazoans were removed from the samples prior to freezing at -40°C . In the laboratory, the samples were freeze-dried and ashed in a low-temperature ashier (LTA) to remove organic matter and concentrate the foraminiferal shells. After ashing, the residue was wet sieved over a 100 μm mesh to remove the ashed organic matter and dry-sieved into two size fractions (150–250 and >250 μm) for foraminiferal census counts. Large samples were split by an Otto dry splitter. On average 351 specimens (170 to 926) were counted per depth interval. For *Globigerinoides trilobus* only the specimens without a sac-like final chamber were considered.

2.2. Sediment Traps

[5] At the CWR site (Figure 1) a Technicap PPS5 sediment trap with a 1 m^2 collecting area and 24 sampling cups was moored at 2 m above the seafloor, at the water depth of 2700 m. The trap was deployed in February 2000, serviced in July 2000 and recovered in February 2001, providing a semicontinuous 1-year record of undisturbed deep-sea deposition flux [*Lončarić et al.*, 2005 also Seasonal export and sediment preservation of diatom, foraminiferal and biogenic mass fluxes in a trophic gradient across the SE Atlantic, submitted to *Progress in Oceanography*, 2006, hereinafter referred to as Lončarić et al., submitted manuscript, 2006]. Prior to mooring, the sample cups were filled with a HgCl_2 -poisoned and Borax-buffered solution in seawater collected from the deployment depth. After trap recovery the samples were stored at 4°C . In the laboratory they were wet-split into at least two aliquots using a Folsom splitter [*Sell and Evans*, 1982; *Griffiths et al.*, 1984]. One aliquot was wet-sieved over 150 μm mesh, rinsed with ethanol, ashed in a LTA and then dry-sieved over a 250 μm mesh to obtain two size fractions for the foraminiferal studies. The first deployment provided an integrated half-a-year sample, whereas the second yielded a complete record with an 8-day sampling resolution. The samples were analyzed individually and afterward pooled into one annual value for comparison with sediment.

2.3. Box Core

[6] The box core 174P03-6 with a 43 cm sediment recovery was taken at the CWR site during the MARE III cruise (February 2001). The sediment was subsampled onboard directly after recovery by two 50 cm long plastic liners, one of which was later subsampled for ^{14}C and ^{210}Pb analyses by syringes (5 cm^3 ; $\phi = 1$ cm) at 1 cm depth interval. These analyses showed that the topmost sediment at the CWR site is modern in age and mixing rates are very low [*Lončarić*, 2005]. The remaining upper 0.5 cm of the core was sampled for foraminiferal analyses and kept frozen at -40°C . In the laboratory, the samples were freeze-dried and sieved into 150–250 and >250 μm fractions.

2.4. Hydrographic Observations

[7] Prior to each plankton tow cast, the upper water column was profiled by a Neill-Brown CTD rosette sampler operated at JGOFS standards or better [*Veth*, 2000]. Twenty-two water samples collected from the upper 620 m of the water column were poisoned and stored dark in sealed bottles at 4°C . They were later used for $\delta^{18}\text{O}$ analysis of seawater ($\delta^{18}\text{O}_w$). CTD-measured temperature, salinity, fluorescence and nutrient concentration were used to characterize water column properties in summer 2000, winter 2000, and summer 2001. Between the in situ observations, SST was obtained from the NOAA remote sensing records for this site, with a 50 km resolution, derived from 8 km resolution global sea surface temperature observations (POES AVHRR/HIRS), tuned to the in situ data at 1 m depth (<http://www.osdpd.noaa.gov>) and compared with our CWR measurements. SeaWiFS remote sensing provided the surface water chlorophyll *a* concentration at 27°S , 4°E . The average

Table 1. Sampling Details of the Plankton Tows Collected at the Central Walvis Ridge Site for Each MARE Cruise^a

Station	Date	Latitude Begin/End	Longitude Begin/End	Tow Interval, m	Volume m ³
<i>MARE 0 (Summer) Cruise</i>					
154 P 03a	19 Feb 2000	27°1.01'S/27°6.01'S	3°52.13'E/3°55.65'E	804–503	669
				503–306	806
				306–155	421
				155–105	129
154 P 03d	19 Feb 2000	27°0.29'S/27°0.91'S	3°51.17'E/3°51.88'E	107–77	73
				77–55	55
				55–29	74
				29–13	32
				13–0	18
<i>MARE II (Winter) Cruise</i>					
1086	30 Jul 2000	27°0.61'S/26°57.71'S	3°51.18'E/3°58.26'E	998–499	972
				499–300	576
				300–202	255
				202–152	143
1089	30 Jul 2000	26°57.81'S/26°58.84'S	3°58.02'E/3°55.93'E	148–100	176
				100–75	112
				75–52	107
				52–24	91
				24–0	115
<i>MARE III (Summer) Cruise</i>					
174 P 03-1	2 Feb 2001	27°0.87'S/27°4.10s	3°51.51'E/3°56.40'E	803–501	575
				501–302	827
				302–201	197
				201–148	148
174 P 03-4	2 Feb 2001	27°0.77'S/27°0.88'S	3°51.71'E/3°51.86'E	154–100	113
				100–74	110
				74–51	92
				51–26	54
				26–0	98

^aCWR, Central Walvis Ridge; MARE, Mixing of *Agulhas* Rings Experiment.

depth of the surface mixed layer (SML) between the CTD measurements was taken from *Levitus and Boyer* [1994] (<http://ingrid.ldeo.columbia.edu/SOURCES/LEVITUS>).

3. Methods

3.1. Foraminiferal Productive Zone and Export Flux

[8] Previous studies on field collected planktic foraminifera show that the shell concentrations profiles have a characteristic pattern [e.g., *Bijma et al.*, 1990; *Oberhänsli et al.*, 1992; *Bijma and Hemleben*, 1994; *Bijma et al.*, 1994; *Ortiz et al.*, 1995; *Peeters and Brummer*, 2002; *Field*, 2004]. In general, concentrations are relatively high in the upper part of the water column, where the foraminifera mainly live, and low at greater depth. This characteristic pattern of decreasing shell concentrations with depth can be used to identify its depth habitat, i.e., the productive zone [e.g., *Berger and Soutar*, 1967; *Peeters and Brummer*, 2002]. We define the base of the productive zone (Z_{BPZ}) for each planktic foraminiferal species at the depth where the concentration profile attains an approximately constant value (Figure 2a) [*Peeters and Brummer*, 2002]. Foraminifera collected above the Z_{BPZ} are considered living and reflect the standing stock (SS). Below Z_{BPZ} concentrations are considered to represent only the remnant shells of dead specimens settling to the seafloor [*Schiebel and Hemleben*,

2000] and are termed export concentration (C_{exp}) (Figure 2b). The standing stock (specimens m^{-2}) is given by

$$\sum_{i=1}^N SS_i = C_i(Z_i - Z_{i-1}) \quad (1)$$

where C_i is the shell concentration (specimens m^{-3}) for the interval i , and Z_i and Z_{i-1} are the start and end depth (m) of each tow interval, respectively (Figure 2a). Since oblique plankton towing through the upper water column per definition integrates foraminiferal concentrations over a depth interval, we derive species standing stocks by addition of all discrete interval concentrations within the productive zone. The value of i ranges from 1 to N , where N is the number of tow intervals within the productive zone. Given the towing technique used, Z_{BPZ} is likely situated somewhere within a towed interval, which combines low concentrations of dead specimens settling to the seafloor and the high pelagic population standing stock measured within the productive zone (Figure 2a). We identify this transition zone as the tow interval between export and productive zone where the upcast shell concentration increases by a factor of two or

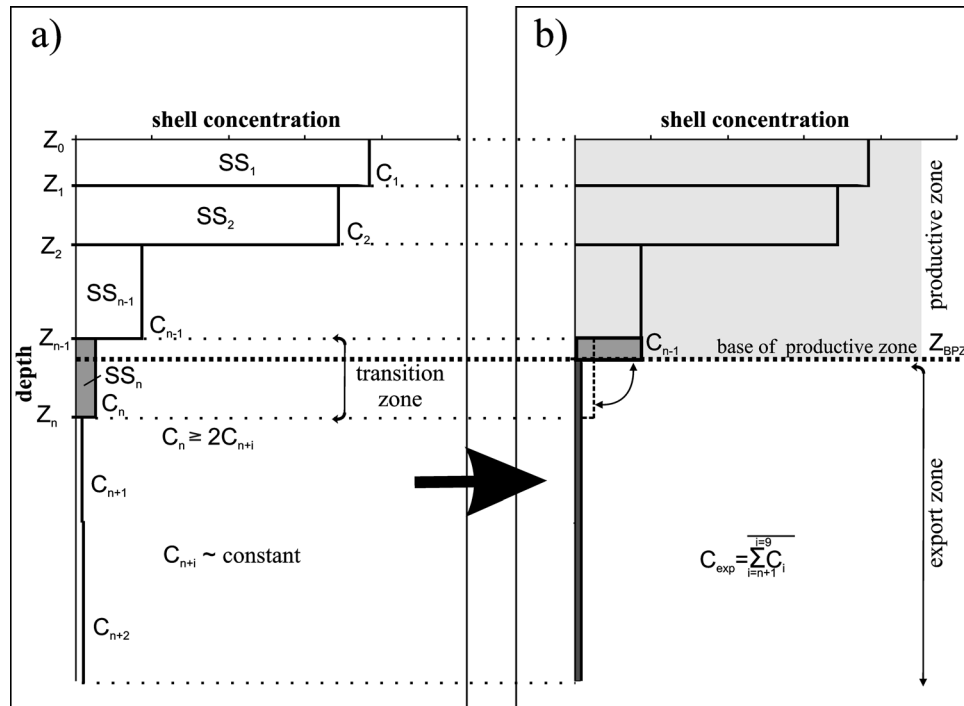


Figure 2. Schematic diagram of a foraminiferal concentration profile in the upper water column illustrating the definition of the base of productive zone (Z_{BPZ}). Shell concentrations (C_n) decrease gradually with depth to an approximately constant value representing only dead specimens (C_{exp}). Foraminifera collected above Z_{BPZ} are considered productive part of the standing stock (SS). In tow intervals across the interface between productive and export zone the shell population is composed of both living and dead (exported) specimens, which after correction for the export population yields Z_{BPZ} . For further explanation, see in text.

higher (Figure 2a). In the transition interval the standing stock (SS_n) is therefore given by

$$SS_n = C_{exp}(Z_n - Z_{n-1}) + C_{n-1}(Z_{BPZ} - Z_{n-1}) \quad (2)$$

where Z_n and Z_{n-1} are the begin and end depth of the transition tow interval (Figure 2b). Since the export concentration of species often has a near, rather than exactly constant value, we follow Peeters and Brummer [2002] and for C_{exp} take the average concentration below the productive zone. Solving for Z_{BPZ} , equations (1) and (2) yield the nominal depth of the base of the productive zone (Figure 2b):

$$Z_{BPZ} = \frac{C_n - C_{exp}}{C_{n-1}}(Z_n - Z_{n-1}) + Z_{n-1} \quad (3)$$

In addition to this definition based on the shell concentration profile, we also define the Z_{BPZ} from the shell $\delta^{18}O$ values measured in each of the plankton tows at the level in the water column at which the $\delta^{18}O_c$ increase cases to attain an approximately constant value. No further increase

of the $\delta^{18}O_c$ with depth is taken as evidence that the species stopped calcifying.

3.2. Oxygen Isotope Analysis

[9] We were able to measure the stable isotope composition of six taxa, i.e., *G. ruber*, *G. trilobus*, *G. glutinata*, left- and right-coiled *G. truncatulinoides* and *G. inflata*. In order to minimize size-related isotope variability, the tests used were microscopically selected according to maximum shell diameter [e.g., Kroon and Darling, 1995]. Tests selected from the fine sieve fraction had a maximum test diameter range of 200 to 300 μm (hereafter referred to as “small”) and from the coarse sieve fraction a maximum diameter range of 350 to 450 μm (“large”), respectively. Specimens selected from the box core surface sediment were cleaned ultrasonically prior to isotope measurement. The box core surface and integrated sediment trap samples were measured in duplicate or triplicate. In total 382 isotope measurements were performed on tests of six planktic foraminiferal species using a Finnigan MAT 252 mass spectrometer equipped with an automated carbonate extraction line at the Vrije Universiteit, Amsterdam (Netherlands). The standard deviation of the external reproducibility was 0.07‰.

[10] The oxygen isotope composition of the seawater ($\delta^{18}O_w$) was analyzed at the University of California, Davis

Table 2. List of Water Samples Analyzed for $\delta^{18}\text{O}_w$ and Used for Linear Regression With Salinity^a

Depth, m	Salinity, ‰	$\delta^{18}\text{O}_w(\text{V-SMOW})$, ‰	Temperature, °C
<i>Station CWR</i>			
18	35.73	0.45	22.20
48	35.76	0.47	18.65
77	35.64	0.41	17.38
95	35.62	0.41	16.31
200	35.26	0.09	13.61
378	34.83	0.11	10.23
501	34.57	-0.02	7.86
617	34.40	-0.26	5.99
<i>Station 154P04</i>			
35	35.89	0.55	21.27
75	35.69	0.50	18.21
95	35.61	0.47	16.94
125	35.55	0.42	16.20
226	35.24	0.35	13.95
300	35.10	0.30	12.63
456	34.79	0.06	9.88
756	34.35	-0.20	7.40
<i>Station 153P22</i>			
29	35.55	0.41	22.83
103	35.45	0.40	18.29
133	35.29	0.36	16.85
226	35.06	0.25	15.72
367	34.71	0.08	14.43
617	34.43	-0.15	13.24

^aSee Figure 3. For station position, see Figure 1.

(Table 2). Following *Craig and Gordon* [1965], we established a linear regression of $\delta^{18}\text{O}_w$ versus salinity in the upper water column (Figure 3):

$$\delta^{18}\text{O}_w(\text{V-SMOW}) = 0.52S - 17.90 \quad (4)$$

Equation (4) was used to obtain continuous depth profiles of $\delta^{18}\text{O}_w$ using the in situ CTD salinity. Isotope values were converted from the V-SMOW to the V-PDB

standard by subtracting 0.27‰ [Hut, 1987]. The equation of *Kim and O'Neil* [1997] was used to calculate the expected equilibrium value for the oxygen isotope composition of calcite ($\delta^{18}\text{O}_{\text{eq}}$). This relationship between temperature, $\delta^{18}\text{O}_{\text{eq}}$ and $\delta^{18}\text{O}_w$ was obtained from precipitation experiments of inorganic calcite and thus excludes life processes like calcification rate [Ortiz *et al.*, 1996], photosynthesis [Spero and Lea, 1993], or respiration [Wolf-Gladrow *et al.*, 1999] but potentially includes the carbonate ion effect [Spero *et al.*, 1997; Bijma *et al.*, 1999; Zeebe, 1999; Russell and Spero, 2000; Peeters *et al.*, 2002]. Since the pH in the experiments of *Kim and O'Neil* [1997] is likely to be lower than the pH of present-day surface waters [Zeebe, 1999], it is also very likely that at least part of the deviations between the Kim and O'Neil equation and living planktic foraminifera is due to changes in ambient pH [Mulitza *et al.*, 2003a]. Following *Kim and O'Neil* [1997],

$$T = 15.2 - 4.6(\delta^{18}\text{O}_{\text{eq}} - \delta^{18}\text{O}_w) + 0.09(\delta^{18}\text{O}_{\text{eq}} - \delta^{18}\text{O}_w)^2 \quad (5)$$

The expected equilibrium can be calculated solving equation (5) for $\delta^{18}\text{O}_{\text{eq}}$, yielding

$$\delta^{18}\text{O}_{\text{eq}} = \delta^{18}\text{O}_w + 25.56 - 3.33\sqrt{T + 43.58} \quad (6)$$

[11] The annual flux-weighted isotope signal $\delta^{18}\text{O}_f$ is calculated as

$$\delta^{18}\text{O}_f = \frac{\sum_{i=1}^N J_i \delta^{18}\text{O}_i}{J_{\text{annual}}} \quad (7)$$

where J_{annual} is the annual flux of a species recorded by sediment traps, J_i is the flux of a particular species recorded by cup i , $\delta^{18}\text{O}_i$ is the foraminiferal isotope composition from

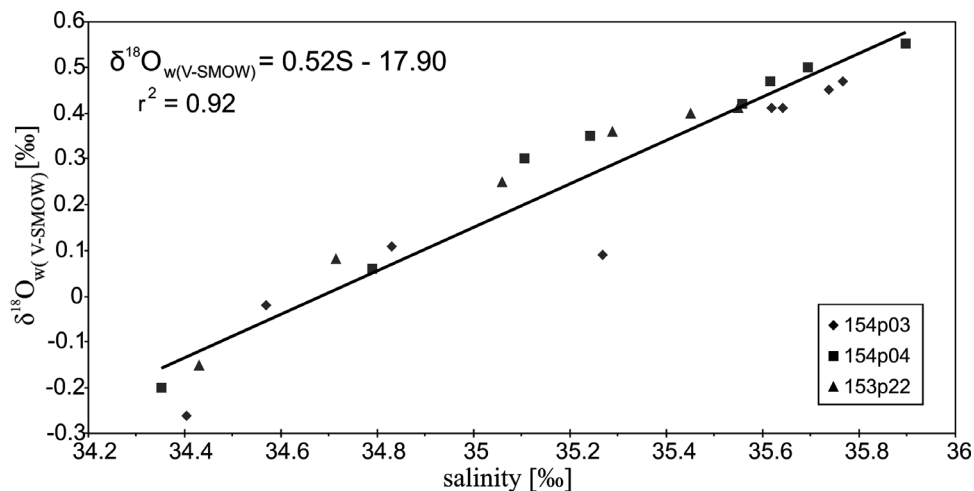


Figure 3. Linear regression of $\delta^{18}\text{O}_w$ versus salinity measured at three sites above the Walvis Ridge (Figure 1).

cup I , and N is the total number of cups. The cups that contained an insufficient amount of foraminiferal carbonate for isotope analysis were not included in the calculations.

4. Results

4.1. Regional Oceanography

[12] Circulation in the central southeast Atlantic Ocean is largely controlled by the Subtropical South Atlantic Gyre. The central Walvis Ridge is under the influence of the eastern flank of this gyre, known as the oceanic branch of the Benguela Current [Peterson and Stramma, 1991; Garzoli and Gordon, 1996]. The CWR site is situated ~1300 km westward from the African continent and the coastal branch of the Benguela Current, associated with the Benguela coastal upwelling system. Although Benguela upwelling belongs to one of the greatest upwelling regions of the world, with filaments of upwelled water reaching hundreds of kilometers offshore, it did not influence the CWR sampling station [Lutjeharms and Stockton, 1987; Shannon and Nelson, 1996; Lončarić, 2005].

[13] The summer 2000 CTD profile was characterized by a sharp shallow thermocline at a depth of 35 m below a SML of 22.2°C (Figure 4a). Yet, the prominent but narrow fluorescence maximum was situated much deeper, at 100 m, just below the nutricline. One year later, in summer 2001, a slightly higher SST was measured (i.e., 22.7°C), but the surface mixed layer fluorescence maximum and nutricline were approximately at the same depth. In contrast to the austral summer profiles, the SML in the austral winter exceeded the depth of 120 m and included the nutricline. The surface water temperature was ~4°C lower and the fluorescence signal was homogeneously distributed over the upper 120 m with a weak maximum at about 110 m, just above the nutricline (Figure 4a).

[14] The SeaWiFS chlorophyll a record revealed predominantly oligotrophic surface water conditions, with increased chlorophyll content at the end of the austral winter (mid-July to September) and mid austral spring (late October) (Figure 4b). The NOAA sea surface temperatures (Figure 4b) ranged from 17°C (austral winter) to 23°C (austral summer) and matched our in situ measurements with an offset of only 0.2°C, 0.0°C, and 0.6°C on 19 February 2000, 30 July 2000, and 2 February 2001, respectively. For the entire period of sampling, radar altimetry imaging (TOPEX/Poseidon) show no perturbations by passing *Agulhas* rings [Lončarić, 2005], i.e., mesoscale eddies of warm-core Indian Ocean waters, which occasionally cross the Walvis Ridge from the proximate Cape Basin [e.g., Lutjeharms, 1996; Schouten et al., 2002]. According to Levitus and Boyer [1994] the average SML at the CWR site was deepest in August (131 m) and shallowest from November through March (26–33 m) (Figure 4b). Our CTD profiles agreed well within a few meters with average Levitus SML depths (Figure 4b).

4.2. Water Column Distribution and Oxygen Isotope Composition of Foraminifera

[15] In this section we present shell concentration and $\delta^{18}\text{O}_c$ profiles that are used to independently estimate the depth of the productive zone in which foraminifera live and calcify, in

contrast to their shell export settling toward the deep ocean floor. For six taxa we address the depth distribution, standing stock and seasonal occurrence, as well as their oxygen isotope composition (Figures 5 and Tables 3 and 4), using two size fractions from the depth-stratified tows collected in summer and winter. These are contrasted with the water column structure in terms of the depth of the SML, seasonal nutricline and chlorophyll a concentration, as obtained from the CTD rosette casts. In order to assess apparent (dis)equilibria between the foraminiferal shell and ambient water, we also consider the in situ equilibrium values for inorganically precipitated calcite [Kim and O'Neil, 1997], using the CTD-measured salinity and temperature, and linear regression of $\delta^{18}\text{O}_w$ (equation (4)).

4.2.1. *Globigerinoides trilobus*

[16] Although rare in winter, *G. trilobus* was abundant in both summer profiles and typically showed highest concentrations near the surface and a rapid decline with depth (Figure 5a). The relative abundance of large shells increased continuously with the depth through the productive zone, from 15% to 58% in summer 2000 and from 8% to 20% in summer 2001. According to the shell concentration, the base of the productive zone was situated at a depth of ~60 m (Z_{BPZ} ; equation (3)), i.e., 30 m deeper than the base of the SML, but 40–50 m shallower than the chlorophyll maximum around the seasonal thermocline. With a Z_{BPZ} of only 60 m, *G. trilobus* stands out as the shallowest of all species, with a standing stock of 662 specimens m^{-2} in summer 2000 and 208 specimens m^{-2} in 2001.

[17] In all profiles *G. trilobus* showed continuously increasing $\delta^{18}\text{O}_c$ value in the upper water column, down to a depth of ~60 m, where it dropped close to a value found at the base of the SML. At greater depth, its $\delta^{18}\text{O}_c$ remained about constant whereas the equilibrium values for ambient water rapidly increased. This demonstrates that the calcification only occurred in the topmost 60 m, well above the DCM and indicates that the shells collected below that level should be considered as the settling export flux. Consequently, the Z_{BPZ} defined by $\delta^{18}\text{O}_c$ was situated at about 60 m, identical to the depth estimate derived from the concentration profiles. Within the SML, *G. trilobus* showed a negative offset of -0.15 to -0.36‰ and -0.13 to -0.18‰ with respect to equilibrium calcification for small and large specimens, respectively (Table 4). Remarkably, the absolute 0.20‰ difference between small and large shells was retained down the export zone.

4.2.2. *Globigerinoides ruber*

[18] In contrast to *G. trilobus*, high shell concentrations of *G. ruber* were also found deep below SML and within the seasonal thermocline down to the DCM (Figure 5b). Although the highest concentrations typically occurred in the SML, the concentration-derived Z_{BPZ} extended to 112–147 m and coincided with the base of the DCM. Below Z_{BPZ} , the shell concentrations were approximately constant. Despite the deeper productive zone, the population of *G. ruber* was smaller than the one of *G. trilobus*, with the highest standing stock of 336 specimens m^{-2} in summer 2000.

[19] All $\delta^{18}\text{O}_c$ profiles of *G. ruber* showed continuously increasing values through the upper water column down to the base of DCM, at a depth of ~125 m. Hereinafter the

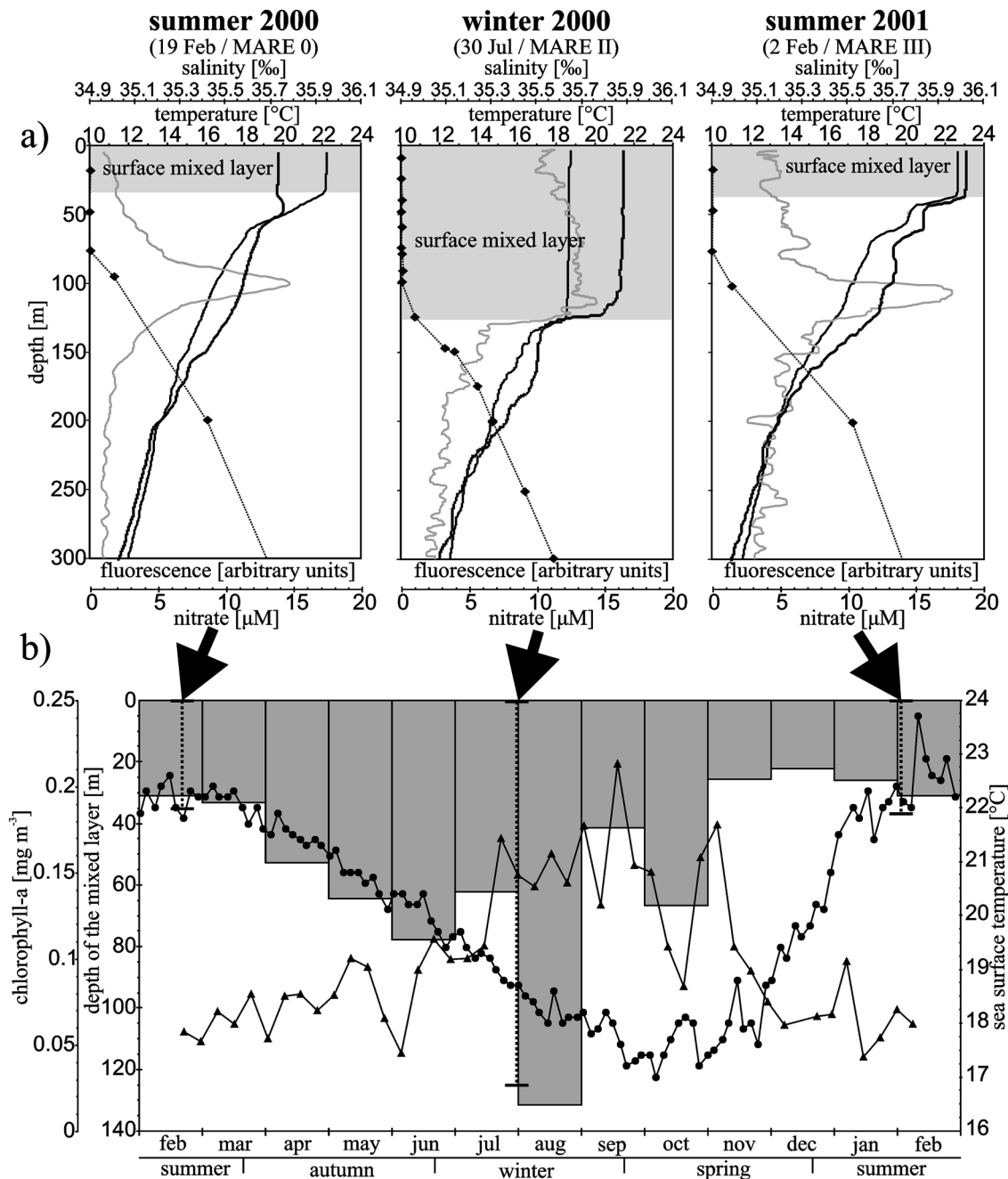


Figure 4. (a) CTD profiles taken at the CWR site in February 2000, July 2000, and February 2001, showing temperature (black line; °C) fluorescence (light gray line; arbitrary units) salinity (dark gray line; ‰), and nitrate concentration (black diamonds; μM) in the upper 300 m of the water column. (b) Satellite-derived sea surface temperature (dots) (NOAA–POES AVHRR/HIRS), and chlorophyll *a* (triangles) (SeaWiFS) for the CWR site from February 2000 to February 2001 and mean depth of the surface mixed layer (gray bars) [Levitus and Boyer, 1994]. Vertical dashed lines mark the CTD and plankton tow sampling (from 4a). The length of the vertical dashed lines corresponds to the CTD measured depths of the surface mixed layer.

$\delta^{18}\text{O}_c$ dropped below values found at the DCM and remained approximately constant regardless rapidly increasing equilibrium values in the ambient water. Thus the $\delta^{18}\text{O}_c$ -derived Z_{BPZ} was situated at about 125 m, well in the range of the Z_{BPZ} as revealed from the shell concentrations.

Within the summer SML, *G. ruber* showed a negative offset with respect to $\delta^{18}\text{O}_{\text{eq}}$ of -0.40 to -0.41‰ and -0.32 to -0.39‰ for the small and large shells, respectively (Table 4). In the deep winter SML, this offset was on average -0.20‰ for the small shells. Notably, the $\delta^{18}\text{O}_c$

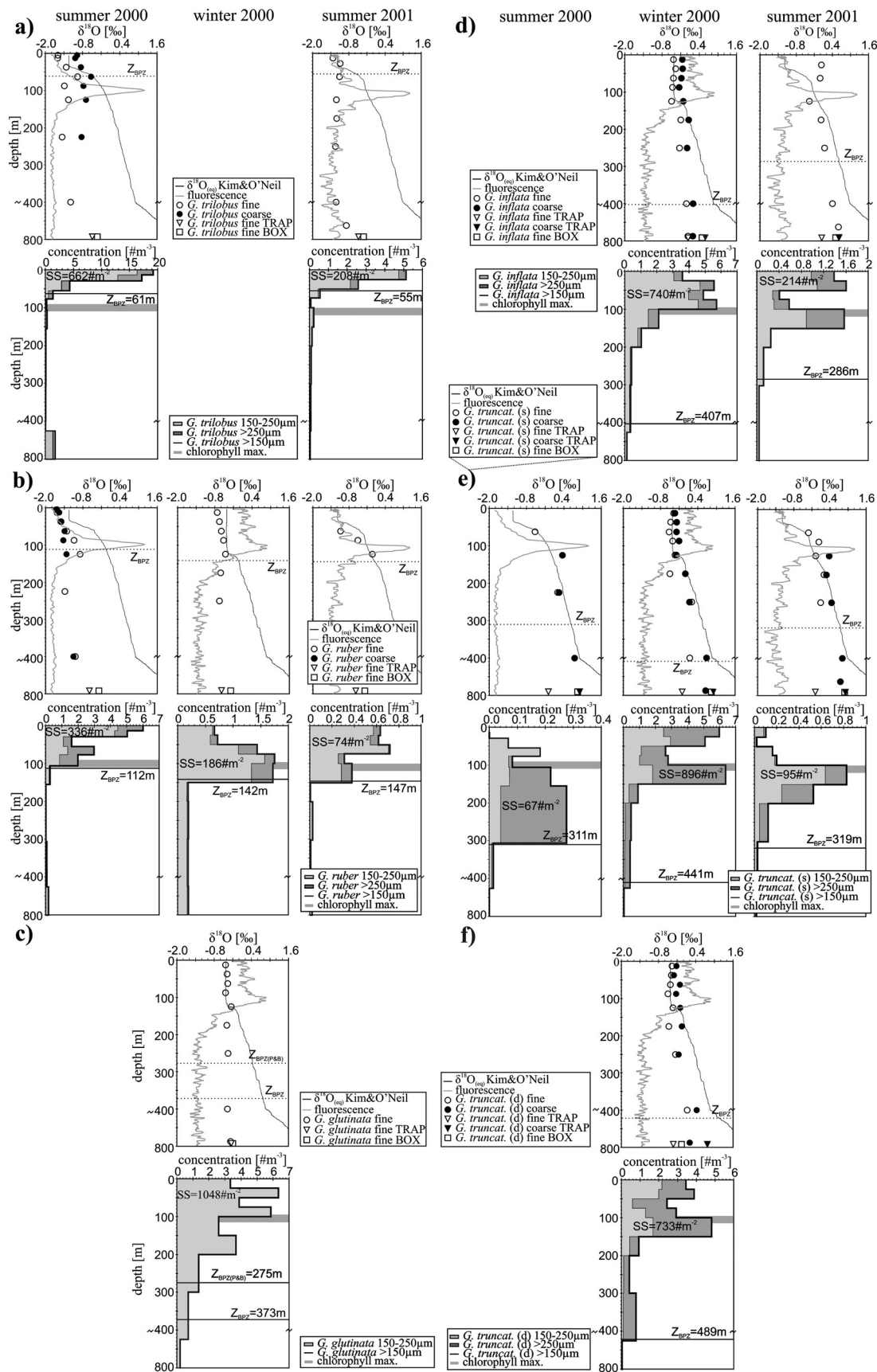


Figure 5

Table 3. The $\delta^{18}\text{O}_c$ Results From the CWR Plankton Tows With Corresponding Expected $\delta^{18}\text{O}_{\text{eq}}$, $\delta^{18}\text{O}_w$, Temperature, and Salinity of Ambient Water

Depth, m	trilobus, ‰		ruber, ‰		glutinata, ‰	inflata, ‰		truncat s, ‰		truncat d, ‰		Kim and O'Neil, ‰	Water $\delta^{18}\text{O}_w$, ‰	Temperature, °C	Salinity, ‰
	Fine	Coarse	Fine	Coarse		Fine	Coarse	Fine	Coarse	Fine	Coarse				
<i>Summer 2000 (MARE 0)</i>															
5	-1.59	-1.37	-1.65	-1.63								-1.24	0.24	22.23	35.72
12.5	-1.60	-1.42	-1.64	-1.56								-1.24	0.24	22.22	35.72
37.5	-1.33	-1.24	-1.50	-1.52								-1.15	0.24	21.77	35.72
62.5	-0.96	-0.92	-1.32	-1.39				-0.53				-0.43	0.20	18.13	35.63
87.5	-1.39	-1.16	-1.08	-1.43								-0.21	0.17	16.97	35.58
125	-1.25	-1.08	-0.89	-1.32					0.36			0.01	0.13	15.76	35.49
225	-1.46	-1.22	-1.37					0.21	0.25			0.38	-0.06	13.21	35.14
400	-1.18		-1.05	-1.10					0.76			0.90	-0.23	10.09	34.79
650												1.75	-0.46	5.46	34.35
<i>Winter 2000 (MARE II)</i>															
12.5			-0.73		-0.43	-0.42	-0.14	-0.37	-0.32	-0.37	-0.22	-0.42	0.33	18.70	35.88
37.5			-0.65		-0.38	-0.36	-0.13	-0.47	-0.28	-0.39	-0.31	-0.42	0.33	18.71	35.88
62.5			-0.59		-0.35	-0.43	-0.17	-0.52	-0.29	-0.42	-0.12	-0.43	0.33	18.71	35.88
87.5			-0.52		-0.43	-0.46	-0.24	-0.41	-0.22	-0.50	-0.24	-0.42	0.32	18.67	35.87
125			-0.46		-0.24	-0.49	-0.11	-0.34	-0.31	-0.34	-0.10	-0.27	0.22	17.45	35.67
175			-0.62		-0.39	-0.19	0.06	-0.50	0.00	-0.47	-0.05	0.05	0.12	15.53	35.48
250			-0.65		-0.35	-0.24	0.01	0.20	0.14	-0.26	-0.15	0.37	-0.04	13.34	35.18
400					-0.37	-0.02	0.20	0.14	0.68	0.13	0.43	0.86	-0.21	10.39	34.84
750					-0.27	0.04	0.19		0.65		0.20	1.93	-0.44	4.78	34.39
<i>Summer 2001 (MARE III)</i>															
12.5	-1.33											-1.18	0.40	22.73	36.03
27.5	-1.09					0.03						-1.18	0.40	22.70	36.03
62.5	-1.10		-1.08			-0.01		-0.31				-0.43	0.25	18.40	35.74
87.5			-0.51					0.03				-0.26	0.24	17.53	35.71
125	-1.22		-0.02			-0.36		-0.08	0.37			-0.08	0.19	16.45	35.62
175	-1.21					0.03		0.22	0.28			0.26	0.02	14.12	35.29
250	-1.25					0.14		0.09	0.46			0.50	-0.08	12.55	35.10
400	-1.23					0.40			0.81			0.99	-0.25	9.65	34.76
650	-0.89					0.60			0.75			1.79	-0.46	5.31	34.36

increase through the upper water column always extended to the DCM, regardless the depth of the SML and the associated thermocline. By contrast to all other species, only for *G. ruber* we measured higher $\delta^{18}\text{O}_c$ values in the small rather than in the corresponding large shell fraction (Table 3).

4.2.3. *Globigerinita glutinata*

[20] This species was found almost exclusively in austral winter, in the size fraction smaller than 250 μm (Figure 5c). Very high standing stock with more than 1000 specimens m^{-2} resulted from the high concentrations recorded throughout the deep SML, where two maxima coincided with fluorescence peaks, but also from the unusually low concentration decrease with depth, which contributed to the deep estimate for the Z_{BPZ} at ~ 370 m. The approach of *Peeters and Brummer* [2002] for determination of Z_{BPZ} , which is based on fitting of foraminiferal average concentrations by Gaussian distribution and defined at two stan-

dard deviations below the depth of maximum concentration predicted by curve fitting, also resulted in a deep estimate of the Z_{BPZ} at ~ 275 m (Figure 5c).

[21] In contrast to the concentration profile, the $\delta^{18}\text{O}_c$ profile of *G. glutinata* was very consistent and suggested a much shallower calcification zone extending from the SML to the top of the seasonal thermocline at ~ 150 m. In the upper four tows collected within the winter SML, the $\delta^{18}\text{O}_c$ closely agreed with the expected $\delta^{18}\text{O}_{\text{eq}}$ (Figure 5c and Table 4). Below 150 m depth, the shell $\delta^{18}\text{O}_c$ was approximately constant and on average 0.06‰ (below analytical precision) higher than the SML value.

4.2.4. *Globorotalia inflata*

[22] The standing stock of *G. inflata* was higher in winter 2000, where shell concentrations closely resembled the fluorescence signal with a double maximum within SML, in contrast to summer 2001 where it had two separate

Figure 5. (top) Oxygen isotope composition and (bottom) foraminiferal shell concentration given in two size fractions, in the upper 800 m of the water column at the CWR site for (a) *G. trilobus*; (b) *G. ruber*; (c) *G. glutinata*; (d) *G. inflata*; (e) *G. truncatulinoides* (sin); and (f) *G. truncatulinoides* (dex). The gray line in the top panels and horizontal gray bars in the bottom panels mark the chlorophyll maximum zone. The core top (squares) and the flux-weighted annual $\delta^{18}\text{O}_c$ (triangles) are given at the base of the isotope panel. The depth of the base of the productive zone (Z_{BPZ}) is derived from the concentration profiles by equation (3). Note change of the vertical scale at 400 m.

Table 4. Shell Oxygen Isotope Disequilibrium Relative to the *Kim and O'Neil* [1997] Equation Measured for Two Test Size Fractions

Species	Offset From Equilibrium for Maximum Test Diameter, ‰	
	200–300 μm	350–450 μm
<i>G. ruber</i> ^a	–0.20 to –0.41	–0.32 to –0.39
<i>G. trilobus</i> ^a	–0.36 to –0.03	–0.13 to –0.16
<i>G. glutinata</i> ^a	+0.02	
<i>G. truncatulinoides</i> (s) ^b	–0.10 to 0.00	–0.14 to +0.01
<i>G. truncatulinoides</i> (d) ^b	0.00	–0.10 to +0.16
<i>G. inflata</i> ^b	+0.02	+0.01 to +0.25

^aDisequilibrium is determined within the surface mixed layer.

^bDisequilibrium is determined approximately at the depth level where shell concentrations were maximal.

maxima at the base of the SML and around the DCM. The concentration decrease below the DCM was not as rapid as for *G. ruber*, therefore suggesting that the base of the productive zone be situated between 300 m in summer and 400 m in winter (Figure 5d).

[23] Winter $\delta^{18}\text{O}_c$ profiles showed approximately constant values within the SML down to the DCM, increasing below it to a depth of ~ 400 m. This demonstrates that the shell calcification ceased below 400 m, which agrees with the depth estimate of the productive zone derived from the concentration profile. Small specimens calcified in equilibrium within the SML, in the zone of maximum concentration, whereas large specimens were in equilibrium between 100 and 200 m depth. The absolute difference between small and large specimens of $0.25 \pm 0.06\text{‰}$ was remarkably constant in the productive and export zones. Two summer tows collected above the DCM showed increased $\delta^{18}\text{O}_c$ values that correspond to the equilibrium values at ~ 150 m and may be related to vertical migration.

4.2.5. *Globorotalia truncatulinoides*

[24] Shell counts and isotope measurements were performed separately for the left- and right-coiled variety. For the left-coiled specimens an increase in the test size with depth has been observed in all concentration profiles (Figure 5e). The maximum abundance of large specimens was found consistently below the SML, in or below the DCM. By contrast, the small specimens showed highest concentrations above or at the DCM. The base of the productive zone, as defined by shell concentrations, was found below 300 m in summer and at ~ 440 m in winter, when the standing stock was higher by an order of magnitude.

[25] In both size fractions the $\delta^{18}\text{O}_c$ of *G. truncatulinoides* (sin) was identical (winter 2000 and summer 2001) or very close (summer 2000) to the expected $\delta^{18}\text{O}_{\text{eq}}$ at the depths of maximum shell concentration (Figure 5e and Table 4). Above these depths large specimens showed $\delta^{18}\text{O}_c$ higher than expected $\delta^{18}\text{O}_{\text{eq}}$, whereas below them the $\delta^{18}\text{O}_c$ followed the expected $\delta^{18}\text{O}_{\text{eq}}$ with a negative offset, demonstrating that the calcification zone extended to 400 m. Consequently, the $\delta^{18}\text{O}_c$ -derived Z_{BPZ} was within the range of the depth estimate derived from the concentration profiles. By contrast, the $\delta^{18}\text{O}_c$ of the fine fraction was approximately constant below 250 m in winter and 175 m

in summer. This indicates that the calcification of the test fraction 200–300 μm ceased shallower than the fraction 350–450 μm and that the export $\delta^{18}\text{O}_c$ of small and large specimens originated from different depths in the water column.

[26] Although absent in summer, right-coiled *G. truncatulinoides* showed high winter standing stock of 730 specimens m^{-2} , with concentrations resembling the left-coiled variety in magnitude and vertical distribution. According to the concentration profiles, the base of the productive zone was situated at a depth of ~ 490 m (Figure 5f). This was the deepest Z_{BPZ} estimate of all species. Similar to left-coiled variety, the $\delta^{18}\text{O}_c$ of right-coiled *G. truncatulinoides* was approximately equal to the expected $\delta^{18}\text{O}_{\text{eq}}$ in the zones of maximum shell concentration. The $\delta^{18}\text{O}_c$ profile suggests that calcification ceased below 400 m, which is in agreement with the concentration-derived Z_{BPZ} .

4.3. Sediment Traps and Core Top Sediment

[27] The annual flux of species was recorded in the sediment trap and yielded the annual $\delta^{18}\text{O}_c$ export signal (equation (7)), which can be compared with the $\delta^{18}\text{O}_c$ signal in the core top sediment (Figure 5 and Table 5). All deep dwellers showed significant difference between the size fractions in the trap $\delta^{18}\text{O}_c$ record. Large specimens, of both left- and right-coiling *G. truncatulinoides*, were 1.0‰ heavier than the corresponding fine ones, where for *G. inflata* the difference amounted to +0.55‰ (Table 5). The seafloor $\delta^{18}\text{O}_c$ (measured only on the small fraction) that represents centennials average (Lončarić et al., submitted manuscript, 2006) was consistently heavier than in the corresponding average deposition flux ($\Delta\delta^{18}\text{O}_c$ in Table 5). The difference was more pronounced for the deep dwellers *G. truncatulinoides* and *G. inflata* than for the shallow dwellers *G. trilobus* and *G. ruber*. The $\Delta\delta^{18}\text{O}_c$ for *G. glutinata* of only +0.03‰ was insignificant, i.e., below the analytical precision.

[28] The winter profile of *G. glutinata* showed the best agreement between the $\delta^{18}\text{O}_c$ of the export flux recovered by the deep plankton tows, the average deposition flux from the sediment trap and the surface sediment from the box core (Figure 5c). Three $\delta^{18}\text{O}_c$ values differ by only $\pm 0.07\text{‰}$, just within the analytical error. Other species that showed a good agreement between the tow export flux $\delta^{18}\text{O}_c$ and the trap annual $\delta^{18}\text{O}_c$ are the large fraction of left-coiled *G. truncatulinoides* in all tow profiles and fine fractions of *G. ruber* and *G. inflata* in winter tow profiles (Table 5).

5. Discussion

5.1. Foraminiferal Productive Zone

[29] The productive zone is the part of the upper water column where planktic foraminiferal species live, calcify and generate the shell export which supplies the sedimentary record. We have used two independent methods to deduce the lower limit of the productive zone Z_{BPZ} for individual species, i.e., from the shell concentrations by equation (3) and from the $\delta^{18}\text{O}_c$ as the depth where shell growth ceases and $\delta^{18}\text{O}_c$ attains approximately constant value. In the analyzed profiles, the $\delta^{18}\text{O}_c$ increased approximately till the Z_{BPZ} as predicted from the concentration

Table 5. Annual Flux Weighted and Centennial Mean $\delta^{18}\text{O}_c$ of Planktic Foraminifera at the CWR Site^a

Species	Annual Flux-Weighted $\delta^{18}\text{O}_c$ (Sediment Traps)		Centennial Average $\delta^{18}\text{O}_c$ (Sediment Surface)	$\Delta\delta^{18}\text{O}$ ~250 μm (Box Trap)
	~250 μm	~400 μm	~250 μm (Average)	
<i>G. truncatulinoides</i> (s)	-0.10	0.91	0.84	0.94
<i>G. truncatulinoides</i> (d)	-0.32	0.77	-0.07	0.25
<i>G. inflata</i>	0.04	0.59	0.49	0.45
<i>G. trilobus</i>	-0.48		-0.32	0.16
<i>G. ruber</i>	-0.59		-0.29	0.30
<i>G. glutinata</i>	-0.23		-0.20	0.03

^a $\Delta\delta^{18}\text{O}$ is the difference between box core top and sediment trap results for the ~250 μm fraction.

profiles, which implies that the two independent approaches for the determination of the Z_{BPZ} generally agreed well. Consequently, both shell concentration and $\delta^{18}\text{O}_c$ can be used confidently to determine the depth range of the foraminiferal productive zone for different species. However, the shell concentration is more dependent on the species population dynamic and therefore may be biased by the moment of sampling (e.g., CWR winter profile of *G. glutinata*), whereas the $\delta^{18}\text{O}_c$ represents an integrated signal. In addition, the precision of Z_{BPZ} estimates is

influenced by the plankton tows depth resolution, which is due to the nature of Multinet sampling lower for the deep intervals, where plankton concentration is low and higher closer to the ocean surface abundant in plankton. The CWR $\delta^{18}\text{O}_c$ patterns suggest that foraminifera indeed grow, add chambers and/or thicken their walls over the entire productive zone as established from the concentration profiles. The depth reconstructed from the $\delta^{18}\text{O}_c$ of exported shells below productive zone and in the sediments therefore represents

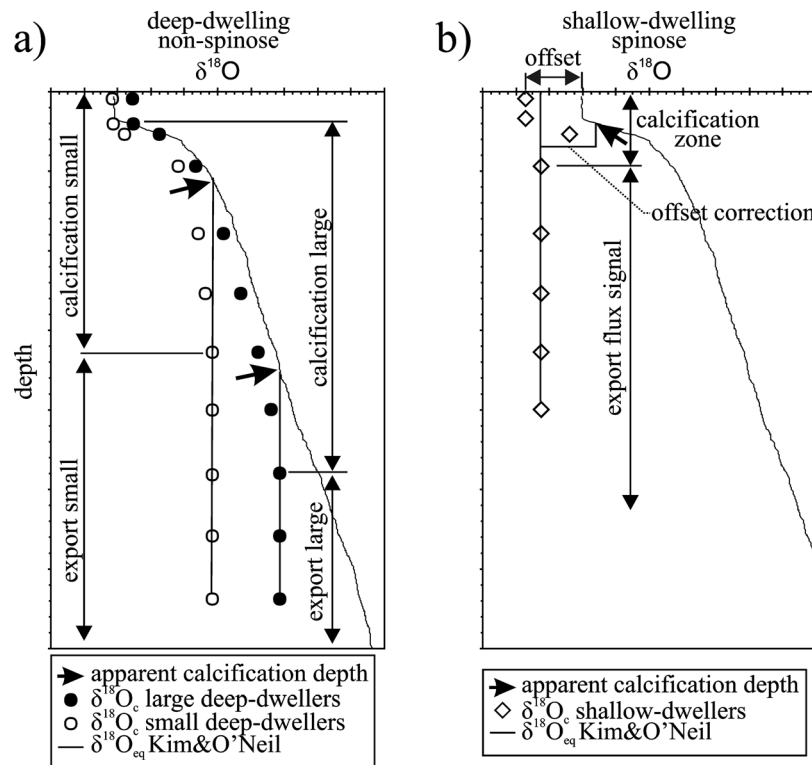


Figure 6. Schematic representation of the $\delta^{18}\text{O}_c$ of (a) deep-dwelling nonspinose (e.g., *G. truncatulinoides* and *G. inflata*) and (b) shallow-dwelling spinose species (e.g., *G. ruber* and *G. trilobus*) in the upper ocean. Nonspinose species calcify in oxygen isotope equilibrium in the zone of maximum concentration, while spinose ones show a negative offset. Most deep dwellers calcify throughout the entire productive zone and therefore is their export $\delta^{18}\text{O}_c$ identical to $\delta^{18}\text{O}_c$ at the Z_{BPZ} . By contrast, only a small part of shallow dwellers calcifies until their Z_{BPZ} . Consequently, their export flux is mixture of shells formed exclusively in the SML and those that continued with calcification within seasonal thermocline. Note the difference between the apparent calcification depth deduced from the export $\delta^{18}\text{O}_c$ and the corresponding depth of the calcification zone.

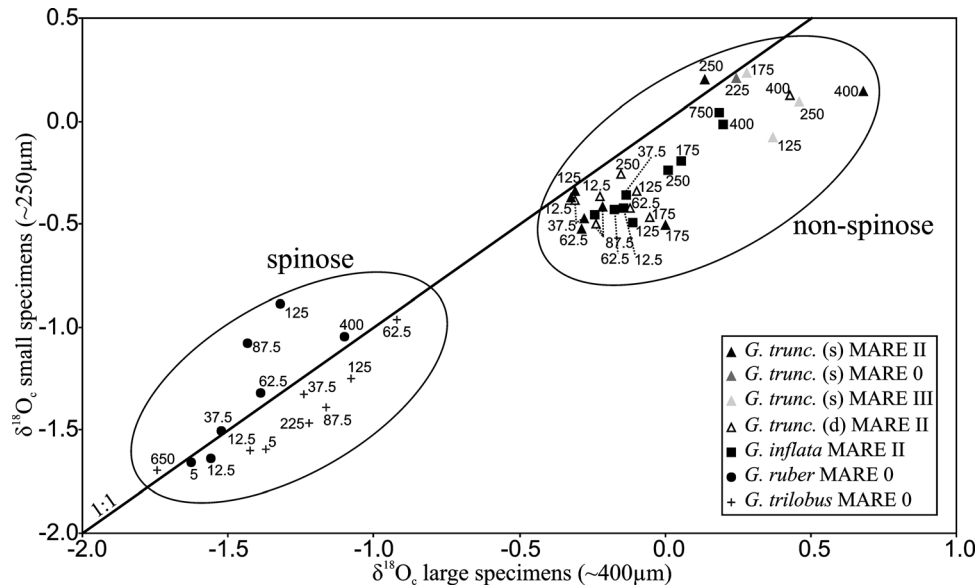


Figure 7. Relationship between $\delta^{18}\text{O}_e$ of small and large shells from the plankton tows at corresponding depth intervals. Large tests are isotopically heavier than the small ones for all species except deep *G. ruber*. Labels refer to the midpoint tow depth interval.

the apparent calcification depth, which integrates the entire calcification cycle of the species (Figure 6).

[30] The shallowest-dwelling species was *G. trilobus* with the Z_{BPZ} around 60 m and highest concentration near the surface, within the summer SML. Interestingly, we observed the productive zone of *G. ruber* to be consistently 50–90 m deeper than for *G. trilobus*. This species is generally considered as shallow dwelling [e.g., Duplessy et al., 1981; Ravelo and Fairbanks, 1992; Niebler et al., 1999, Field, 2004] and a good indicator of the near-surface conditions [Hemleben et al., 1989]. Rather than confined to the SML, at the CWR the productive zone of *G. ruber* extends down to the DCM, with the Z_{BPZ} between 110 and 150 m (Figure 5b). Although different from e.g., studies of Deuser and Ross [1989] (Sargasso Sea) and Kemle-von Mücke and Oberhänsli [1999] (eastern equatorial South Atlantic), such maxima of *G. ruber* at the DCM have already been reported elsewhere [e.g., Fairbanks and Wiebe, 1980; Peeters et al., 2002]. Thus, at the sites with a “typical tropical ocean” structure [Herbland and Voituriez, 1979; Mann and Lazier, 1991], where a shallow SML is well developed and separated from the DCM, *G. ruber* only partly reflects the SML conditions. The deepest-dwelling taxa at the CWR site were *G. truncatulinoides* and *G. inflata*, with the Z_{BPZ} ranging between 310 and 490 m (Figures 5e and 5f) and 290 to 410 m (Figure 5d), respectively. Although concentration profiles of *G. inflata* resulted in a somewhat shallower Z_{BPZ} than for left- and right-coiled *G. truncatulinoides*, its $\delta^{18}\text{O}_e$ profiles suggest similar productive zones extending to ~400 m. Generally, shallow dwellers *G. ruber* and *G. trilobus* showed a better match between two Z_{BPZ} approaches than deep dwellers *G. inflata* and *G. truncatulinoides*, which can be attributed to the higher resolution of shallow tow intervals. The only mismatch was observed for the Z_{BPZ} of *G. glutinata* (Figure 5c); the concentration profile situates the Z_{BPZ} at

370 m, or at 275 m using the approach of Peeters and Brummer [2002], whereas the $\delta^{18}\text{O}_e$ profile suggests a much shallower productive zone. Such discrepancy may arise from a number of factors such as the state of population dynamics or vertical migration. The $\delta^{18}\text{O}_e$ data, however, strongly suggest that the Z_{BPZ} of *G. glutinata* is not deeper than 130–150 m.

5.2. Species-Specific and Size-Related $\delta^{18}\text{O}_e$ Changes

[31] Oxygen isotope analyses of living foraminifera demonstrate species-specific offsets, where spinose species usually show larger negative offset from the expected $\delta^{18}\text{O}_{\text{eq}}$ than the nonspinose species (in agreement with previous observations, e.g., Fairbanks et al. [1980]). In addition, planktic foraminifera commonly show a lower $\delta^{18}\text{O}_e$ in small specimens than measured for large ones of the same species (Figure 7) [Erez and Honjo, 1981; Kroon, 1988]. Such $\delta^{18}\text{O}_e$ differences are also observed at the CWR, where size-related effect has been attributed to a growth at different depth and hence different calcification temperature, but may also be caused by ontogenic altering of the $\delta^{18}\text{O}_e$ composition during growth [Kroon and Darling, 1995; Bemis et al., 1998]. Spinose species usually contain symbiotic algae [Hemleben et al., 1989]. Their high photosynthetic rate results in higher CO_2 fixation which further causes increase of ambient pH and carbonate ion $[\text{CO}_3^{2-}]$ concentration [Bijma et al., 1999]. Since increasing pH results in decreasing $\delta^{18}\text{O}$ of the foraminiferal calcite [Spero et al., 1997; Zeebe, 1999; Bijma et al., 1999], specimens containing more symbionts or growing closer to the surface under maximum light intensity should be depleted in $\delta^{18}\text{O}$.

[32] For all spinose species at the CWR site we observed a negative $\delta^{18}\text{O}_e$ offset with respect to the expected $\delta^{18}\text{O}_{\text{eq}}$ (Figure 6). *G. ruber* showed the offset value of -0.4‰ to -0.2‰ within the mixed layer during both seasons

Table 6. Temperature Equation Used in This Study and Published Prior to 1997^a

Reference	T = a + b($\Delta\delta^{18}\text{O}_f$) + c($\Delta\delta^{18}\text{O}_f$) ²		
	a	b	c
Kim and O'Neil [1997]	15.2	-4.6	0.09
Epstein et al. [1953]	16.4	-4.2	0.13
Craig [1965]	16.9	-4.2	0.13
Shackleton [1974]	16.9	-4.38	0.1
Erez and Luz [1983]	17.0	-4.52	0.03

^aThe oxygen isotopic composition of foraminifera is expressed as $\Delta\delta^{18}\text{O}_f$ and equals the difference between the shell and seawater (i.e., $\delta^{18}\text{O}_c - \delta^{18}\text{O}_w$) (equation format after Bemis et al. [1998, 2000]).

(Figure 5b and Table 4). This is within the range reported by Peeters et al. [2002] for the monsoonal-influenced Arabian Sea, as well as by Fairbanks et al. [1980] for the western North Atlantic and by Erez and Honjo [1981] for the central North Atlantic, taking into account the heavier reference equilibrium value (Table 6). For *G. trilobus* we found smaller offsets of -0.15‰ to -0.35‰ within the SML. These agree with findings from the Panama Basin, where Fairbanks et al. [1982] reported in the similarly shallow SML the offset of approximately -0.10 to -0.30‰ , after reference $\delta^{18}\text{O}_{\text{eq}}$ correction.

[33] The CWR summer 2000 concentration profiles for small and large tests of shallow-dwelling *G. trilobus* and *G. ruber* show a similar vertical distribution, both having maximum within the SML (Figure 5). Yet, two size fractions show different $\delta^{18}\text{O}_c$. Small tests of *G. trilobus* have within the summer SML an offset of -0.18 to -0.22‰ relative to the $\delta^{18}\text{O}_c$ from the large shells, whereas *G. ruber* shows only insignificant $\delta^{18}\text{O}_c$ difference between the shell size fractions (Figure 7). Since the calcification environment is the same within the SML, the $\delta^{18}\text{O}_c$ offset between the size fractions of *G. trilobus* has to be of an internal, ontogenic nature. Bemis et al. [1998] showed conclusively for small and large *G. bulloides* that a considerable size $\delta^{18}\text{O}_c$ difference exists. It has been suggested that specimens growing closer to the surface become larger and harbor more symbionts [Spero and Williams, 1988; Spero and Lea, 1993]. Hence, as a result of the symbiont activity their $\delta^{18}\text{O}_c$ should decrease due to the changes in ambient pH. However, we observed in all concentration profiles of *G. trilobus* an increase in relative abundance of larger shells with the depth through the productive zone although its $\delta^{18}\text{O}_c$ decreased toward the surface, an exactly opposite trend than what suggested for *O. universa* [Spero and Williams, 1988] and *G. trilobus* [Spero and Lea, 1993]. Remarkably, difference between small and large *G. trilobus* was retained below the productive zone, indicating that calcification of both fractions at the CWR was largely restricted to the SML. For paleoceanographic applications, it has also to be considered that morphotypes of *G. trilobus* without sac-like final chamber presented in Figure 5a, always occur shallower than those with sac-like chamber at the CWR [Lončarić et al., 2005] and elsewhere [e.g., Erez et al., 1991; Bijma and Hemleben, 1994]. The sac-like chamber is formed within the seasonal thermocline, where also the calcite crust may be added prior the gametogenesis [Lohmann, 1995]. Consequently, the $\delta^{18}\text{O}$ analysis performed on the fossil record of entire population including

two morphotypes would result in significant underestimation of the SST [Spero and Lea, 1993]. Notable $\delta^{18}\text{O}_c$ increase in the *G. ruber* fine fraction down the deep winter SML, from -0.73‰ to -0.46‰ (Figure 5b), suggests an additional controlling mechanism affecting $\delta^{18}\text{O}_c$ within the same fraction and in the same ambient water, which may be related to the symbiont activity under different light conditions [Spero and Lea, 1993], where specimens growing closer to the surface under maximum light intensity become depleted in $\delta^{18}\text{O}_c$ [Bijma et al., 1999]. The exceptionally low $\delta^{18}\text{O}_c$ values of large *G. ruber* in summer 2000 (Figures 5b and 7) could have resulted from temporal migration toward the DCM, or could be a consequence of distinct populations of small specimens (i.e., “cryptic species”) calcifying both within the SML and around the DCM, which is consistent with the CWR concentration profiles and in line with recent DNA studies on planktic foraminifera [e.g., Darling et al., 1996; Huber et al., 1997; Darling et al., 1999].

[34] The oxygen isotope composition of nonspinose species is close to the expected $\delta^{18}\text{O}_{\text{eq}}$ value near the depth where shell concentrations are maximal (Figures 5c–5f and 6). Given that the zone of maximum concentration indicates the preferred depth habitat of the species [Schiebel and Hemleben, 2000] and is the place where most of the foraminiferal calcite is formed [Peeters and Brummer, 2002], then the studied nonspinose species, *G. truncatulinoides*, *G. inflata*, and *G. glutinata* appear to calcify in oxygen isotope equilibrium (Figures 5c–5f). The concentration profiles of deep dwellers, in particular *G. truncatulinoides*, show an increase in test size with depth. Small specimens predominate at shallower depths in the water column and therefore calcify in warmer water, resulting in a lighter shell $\delta^{18}\text{O}_c$. Small specimens from the subsurface calcified larger part of their test in the relatively warm water of the SML, resulting in a negative $\delta^{18}\text{O}_c$ offset compared to large specimens from the same depth interval. Conversely, large specimens found in the SML may have migrated, or were expatriated from greater depth where they calcified most of their shell at higher $\delta^{18}\text{O}_{\text{eq}}$, resulting in a positive $\delta^{18}\text{O}_c$ offset (Figure 6).

5.3. Calcification Temperature Versus $\delta^{18}\text{O}_c$ Export Flux

[35] Plankton towing combined with the CTD profiling attained at the CWR allows for direct comparison of the $\delta^{18}\text{O}_c$ signal from the foraminiferal export zone to the in situ measured temperature applying equation (5) of Kim and O'Neil [1997]. In this section the export $\delta^{18}\text{O}_c$ of spinose *G. ruber* and *G. trilobus* are compared to the measured SST, after correction for the in situ observed offset from the SML. Since the nonspinose *G. glutinata*, *G. truncatulinoides*, and *G. inflata* did not show a significant offset, their export $\delta^{18}\text{O}_c$ is directly compared to the expected $\delta^{18}\text{O}_{\text{eq}}$ profile and recalculated to ambient temperature.

5.3.1. Shallow Dwellers

[36] As previously shown, *G. trilobus* is the shallowest-dwelling species at the CWR, with only few specimens that continue to calcify below the SML, down to ~ 60 m depth. Still, the export $\delta^{18}\text{O}_c$ shows positive shift relative to the

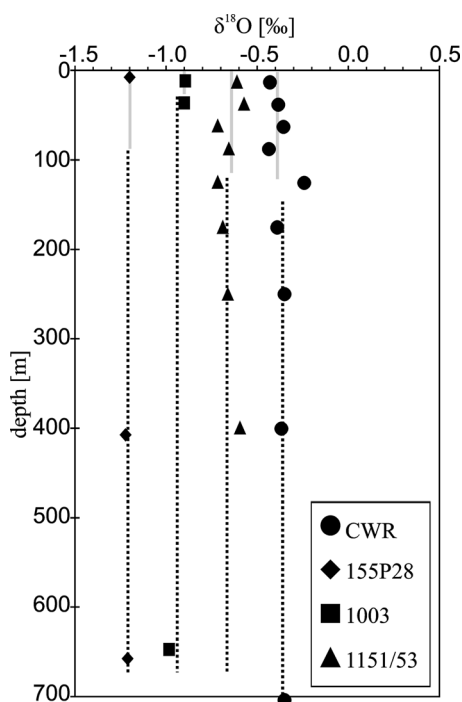


Figure 8. Oxygen isotope composition of *G. glutinata* from plankton tows collected at the CWR site (dots) and elsewhere in the Cape Basin (diamonds, 155P28, 38°1'S, 18°25'E; squares, 1003, 35°56'S, 16°6'E; triangles, 1153, 38°40'S, 13°58'E). Solid grey and stippled black lines represent average $\delta^{18}\text{O}_c$ within the surface mixed layer and below it, respectively.

$\delta^{18}\text{O}_c$ value from the SML with a range of 0.17‰ to 0.28‰ in the fine, and about 0.25‰ in the coarse fraction, respectively. This suggests dynamic behavior of *G. trilobus* that actively migrates within the productive zone between the reproductive depth and the upper photic zone [Hemleben and Bijma, 1994] and forming of additional calcite in colder water. The summer temperature estimates based on the export $\delta^{18}\text{O}_c$ are, after correction for the in situ observed offset, lower than the measured SST, with an underestimate of 0.9 to 1.3°C for the small and $\sim 1.2^\circ\text{C}$ for the large shells.

[37] The CWR tow results indicate the DCM as the level in the water column that borders the productive zone of *G. ruber* and suggest that the calcification extends from the sea surface to the chlorophyll maximum. Both $\delta^{18}\text{O}_c$ and the concentration profiles show surprisingly high numbers of *G. ruber* calcifying always down to 125 m depth where the DCM occurs (Figure 5b). In winter, when the deep SML includes the DCM, the temperature estimate from the export $\delta^{18}\text{O}_c$ of *G. ruber* equals the measured SST. However, in summer when the DCM occurs 60–70 m below the SML, the temperature estimate from *G. ruber* export $\delta^{18}\text{O}_c$ underestimates the in situ SST for 2.1 to 2.4°C for the fine and coarse fraction, respectively. Note that this calculation holds when using the temperature equation of Kim and O'Neil [1997] and with an in situ obtained disequilibrium correction of 0.32 to 0.41‰. Thus, in the “typical tropical ocean” water column structure, where SML and DCM are well

separated, and consequently, the chlorophyll maximum temperature departs significantly from the surface temperatures, the SST estimates based on the export $\delta^{18}\text{O}_c$ of *G. ruber* may be inadequate.

[38] Of the species considered here, the $\delta^{18}\text{O}_c$ record of *G. glutinata* is the most constant throughout the water column (Figures 5c and Table 3). Its winter export $\delta^{18}\text{O}_c$ yields a temperature of 18.4°C, which is only 0.3°C lower than the in situ measured SST. Also elsewhere in the Cape Basin (Figure 8), differences between the average $\delta^{18}\text{O}_c$ of *G. glutinata* within the SML and from its export flux appear identical within the analytical error and the SST is accurately reflected in the $\delta^{18}\text{O}_c$ of exported specimens. Consequently, our findings indicate that *G. glutinata* is a surface dwelling species, and, as such, its shell geochemical fingerprint may provide a robust proxy for past $\delta^{18}\text{O}$ or SST variability.

5.3.2. Deep Dwellers

[39] The deepest-dwelling taxa encountered in this study are right- and left-coiled *G. truncatulinoides* with max. Z_{BPZ} at 490 and 440 m, respectively, as well as *G. inflata* with a Z_{BPZ} at 410 m (Figures 5d–5f). These taxa appear to calcify in oxygen isotopic equilibrium in the zone of maximum shell concentration, which is for the small specimens usually shallower than for the large ones. For the species *G. truncatulinoides*, we calculated that calcite from the 250 μm tests contributes less than 10% of the 400- μm fraction shell mass (Figure 9). Hence, even if the 250 μm test were completely precipitated within the SML, the contribution of that “warm water” calcite in the 400 μm test is very small. Additional argument pointing to only a minor contribution of the calcite from SML to the shells exported from the productive zone is the similarity between the $\delta^{18}\text{O}_c$ of the exported shells and those from the base of the productive zone (Figures 5d–5f and 6a). This suggests that most of the population continues calcification down to Z_{BPZ} where the export $\delta^{18}\text{O}_c$ is generated, in contrast to shallow dwellers, where only smaller part of the population calcifies till Z_{BPZ} (Figure 6). Consequently, we may conclude that *G. truncatulinoides* and *G. inflata* predominantly calcified below the SML. Although large specimens of these taxa occasionally occur within the SML (e.g., in the summer profiles), this has no significant impact on the isotopic composition of exported shells settling to the seafloor. Such population behavior has important consequences for the apparent calcification temperature and depth reconstructed from the exported shells. From the CWR $\delta^{18}\text{O}_c$ profiles it appears that the calcification zone for large specimens of *G. truncatulinoides* and *G. inflata* is ~ 300 m wide and covers the temperature gradient of about 7°C. Yet, in spite the wide calcification zone, the apparent calcification range calculated from export $\delta^{18}\text{O}_c$ is narrow. Left-coiled *G. truncatulinoides* manifests amongst all deep dwellers a most consistent record in contrasting hydrographic seasons (i.e., a summer SML of 35 m vs. winter SML of 125 m). Its apparent calcification depth derived from the export $\delta^{18}\text{O}_c$ coarse fraction spans only 18 m for large specimens, ranging between 335 and 353 m depth, which corresponds to a temperature span of 0.7°C, ranging from 10.8°C to 11.5°C (Table 7). The apparent calcification depth at

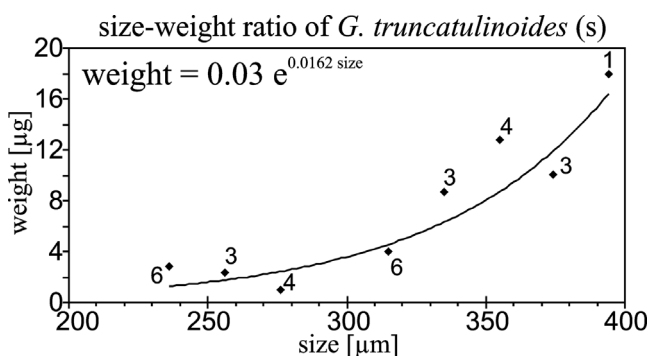


Figure 9. Size-weight relationship of left-coiled *G. truncatulinoides* from the sediment trap at the CWR site. Size refers to the microscopically measured largest test diameter. Because of the low weights and balance limitations, several tests of the same size (labels next to symbols) are lumped together and weighed. Note that the weight of average 400 μm test is more than 11 times higher than the 250 μm test. For more shell size measurements, see Lohmann and Schweitzer [1990].

~ 340 m derived from $\delta^{18}\text{O}_c$ of large *G. truncatulinoides* matches the modeling results (350 m) of *LeGrande et al.* [2004]. Small specimens show warmer and shallower, but comparably narrow apparent calcification intervals (temperature range 14.1°C to 14.7°C; depth range 165 to 202 m). The apparent calcification depth of *G. inflata* varies from ~ 150 –200 m in summer to ~ 250 m in winter. Thus *G. truncatulinoides* and *G. inflata* from the CWR show a wide calcification zone, but a narrow apparent calcification temperature/depth with low seasonal variability. Furthermore, it stands out that the shell size of deep dwellers appears as an important parameter that influences calculated apparent calcification temperatures.

5.4. Seasonality and Annual $\delta^{18}\text{O}_c$

[40] Seasonal and vertical calcification weight the annual $\delta^{18}\text{O}_c$ of a foraminiferal population toward the values associated with hydrographic conditions in the preferred ecological niche [Mulitza *et al.*, 2003b]. The importance of seasonal events for the general sedimentation pattern and the prevailing signal that reaches the sediment can be illustrated by comparison of export $\delta^{18}\text{O}_c$ derived from plankton tows during contrasting seasons with the annual flux-weighted $\delta^{18}\text{O}_c$ derived from near-bottom sediment traps. This provides a valuable link between the modern oceanographic conditions and the information stored in the fossil record.

[41] The best agreement between the export $\delta^{18}\text{O}_c$ and the annual $\delta^{18}\text{O}_c$ is found for *G. glutinata*, which was at the CWR abundant in winter. The calcification temperature calculated from the annual flux $\delta^{18}\text{O}_c$ is 18.3°C, identical to the austral mid winter (late July) and mid spring (October–November) SST (Figure 4b), when its highest flux is recorded at the CWR site [Lončarić, 2005]. Consequently, the annual flux $\delta^{18}\text{O}_c$ of *G. glutinata* provides an excellent proxy for the winter/spring surface temperature in this part of the ocean.

[42] Flux-weighted annual $\delta^{18}\text{O}_c$ of *G. ruber* is identical to the winter plankton tow export $\delta^{18}\text{O}_c$ flux. At the CWR it provided a good estimate of the winter/spring SST, after in situ offset correction. However, as we already showed, if the larger part of its annual flux is deposited in the period of “typical tropical ocean” structure such as in summer at CWR, its $\delta^{18}\text{O}_c$ may underestimate the SST by more than 2°C.

[43] For left-coiled *G. truncatulinoides* we observed a good agreement between the export and annual average $\delta^{18}\text{O}_c$ signals particularly in summer populations. The deposition flux of *G. truncatulinoides* (sin) at the CWR is highest in December and January [Lončarić, 2005], suggesting that most of the annual flux arrives to the seafloor during the austral early summer. This explains why we found a better agreement between the export and annual $\delta^{18}\text{O}_c$ in February rather than July tows. The trap annual $\delta^{18}\text{O}_c$ yielded a temperature of 10.3°C for the depth of 350 m and 15.5°C for the 200 m depth, which is close to the average in situ temperature of 10.8°C and 13.6°C measured by summer CTD profiles. The larger temperature overestimate at about 200 m (+1.9°C) is probably due to the steeper temperature gradient at shallower depths and the fact that the seasonal flux maximum precedes our CTD/plankton tow sampling by 1–2 months. Likely was the average CWR December/January temperature at 200 m depth higher than in situ measured in February 2000 and 2001. The annual $\delta^{18}\text{O}_c$ of *G. inflata* gives a good estimate for the winter sea temperature at about 150 m, which agrees well with the maximum seasonal flux of this species observed at the CWR during winter/spring [Lončarić, 2005].

5.5. Sediment Record

[44] The CWR core top $\delta^{18}\text{O}_c$ values were consistently higher than in the corresponding annual fluxes (Table 5), as commonly observed in the South Atlantic [Mulitza *et al.*,

Table 7. Export $\delta^{18}\text{O}_c$ of *G. truncatulinoides* (sin) From the Summer 2000, Winter 2000, and Summer 2001 Tow Profiles in the Fine and Coarse Size Fractions^a

	Size Fraction		Water	
	$\sim 250 \mu\text{m}$	$\sim 400 \mu\text{m}$	200 m	350 m
	$\delta^{18}\text{O}_c$, ‰			
M 0	0.21	0.76	−0.03	−0.18
M II	0.17	0.67	0.07	−0.15
M III	0.16	0.16	−0.02	−0.19
	T , °C			
M 0	14.1	11.0	13.5	11.0
M II	14.7	11.5	14.8	11.3
M III	14.4	10.8	13.5	10.6
	Z_c , m			
M 0	186		353	
M II	202		341	
M III	165		335	

^aM-0, summer 2000; M-II, winter 2000; and M-III, summer 2001. The corresponding water isotope composition and temperature and resulting estimate for apparent calcification temperature (T) and apparent calcification depth (Z_c) are given. The calcification temperature T is calculated using equation (5). The calcification depth Z_c is the depth at which the calcification temperature T equals the water temperature as measured in situ by CTD.

2003b] and elsewhere [e.g., Duplessy *et al.*, 1981; Erez and Honjo, 1981; Deuser, 1987; Lohmann, 1995]. Differences ($\Delta\delta^{18}\text{O}_c$) were larger for the nonspinose *G. truncatulinoides* (sin) and *G. inflata* than for spinose *G. ruber* and *G. trilobus* (Table 5). For *G. glutinata*, $\Delta\delta^{18}\text{O}_c$ was within the analytical error and its sediment $\delta^{18}\text{O}_c$ accurately reflects the winter/spring SST (Figure 5c and Table 5).

[45] Mulitza *et al.* [2003b] emphasized two primary mechanisms that may account for the observed deviation between the annual mean and core top $\delta^{18}\text{O}_c$: (1) a shell flux biased toward seasons or periods when the ambient temperature was lower than the annual mean or (2) subsurface calcification at lower temperatures. Addition of secondary calcite in waters deeper than where shells normally grow may account for one third or more of a shell's mass [Erez and Honjo, 1981; Schweitzer and Lohmann, 1991]. Since we observed relatively constant export $\delta^{18}\text{O}_c$ in most of the plankton tows, secondary calcification at the CWR takes place below 800–1000 m, either as gametogenic calcification or deep encrustation (Plate 12 of Lončarić [2005] at <https://dare.uvu.vu.nl/bitstream/1871/9103/1/6943.pdf>) of shells in the cold water of the export zone and at the seafloor. In contrast to the trap $\delta^{18}\text{O}_c$ record, which covers one year of deposition of the foraminiferal carbonate at the CWR, the core top $\delta^{18}\text{O}_c$ represents a centennial average, since it takes hundreds of years before actual shell burial across the sediment-water interface (Lončarić *et al.*, submitted manuscript, 2006). Therefore the interannual variability in the seasonal flux may account for the higher core top $\delta^{18}\text{O}_c$, e.g., by the relatively higher flux of deep dwellers in winter, compared to the season 2000–2001.

[46] The foraminiferal isotope signal in the sediment may also be altered by postdepositional processes [e.g., Mulitza *et al.*, 2003b]. Mechanical processes at the sea bottom, such as fragmentation of thin-walled, nonencrusted adult shells with relatively low $\delta^{18}\text{O}_c$, or selective accumulation of heavy (mass and $\delta^{18}\text{O}_c$) specimens, but also differential dissolution related to heterogeneous shell chemistry [e.g., Brummer *et al.*, 1987; Hemleben *et al.*, 1989; Lohmann, 1992, 1995], can result in a positive $\delta^{18}\text{O}_c$ shift. Yet, it is unlikely that the partial dissolution at the CWR affected most severely only the initial chambers of the deep-dwelling, nonspinose species, which are generally characterized by the more robust shells (summarized by Hemleben *et al.* [1989]), leaving in tact relatively delicate tests of *G. glutinata*, *G. trilobus*, and *G. ruber*.

[47] Although at this stage of the research it is difficult to pinpoint the true mechanism causing the observed $\Delta\delta^{18}\text{O}_c$, it is most likely related to the interannual flux changes, perhaps combined with other processes like deep encrustation of deep dwellers, fragmentation of thin-walled calcite or selective accumulation of heavy specimens. Independently

of this, *G. glutinata* stands out as a good proxy of the SST in the CWR surface sediments.

6. Conclusions

[48] In this study, we have used two independent methods to deduce the base of the productive zone for six foraminiferal taxa at the central Walvis Ridge: (1) from the shell concentrations and (2) from the shell $\delta^{18}\text{O}_c$. In the analyzed profiles, two approaches generally agreed well yielding similar Z_{BPZ} . This implies that both shell concentration and $\delta^{18}\text{O}_c$ can be used confidently to determine the depth range of the foraminiferal productive zone for different species.

[49] The species *G. glutinata* appeared to calcify within the surface mixed layer and therefore its geochemical characteristics may serve well as a proxy of the sea surface temperature or other surface ocean chemical/physical parameters. It calcified in equilibrium with the expected $\delta^{18}\text{O}$ and showed constant $\delta^{18}\text{O}_c$ in the export flux recovered by plankton tows, the annual average deposition flux from the sediment traps and the surface sediment from the box core of the same site. In the CWR surface sediment, *G. glutinata* stands out as an excellent proxy of the winter/spring SST, as confirmed by the annual flux-weighted $\delta^{18}\text{O}_c$ and the satellite-derived temperature record.

[50] The annual $\delta^{18}\text{O}_c$ of left-coiled *G. truncatulinoides* provides a good estimate of the summer (December–January) subsurface temperature. The $\delta^{18}\text{O}_c$ from the specimens with a maximum test size of $\sim 400\ \mu\text{m}$ reflects the temperature at about 350 m and those with tests of $\sim 250\ \mu\text{m}$ at about 200 m. Consequently, the $\delta^{18}\text{O}_c$ difference between small and large specimens in the sediment may be used to estimate the subsurface temperature gradient.

[51] The $\delta^{18}\text{O}_c$ record of *G. ruber* from the surface sediment provided a good estimate of the winter SST at the CWR. However, our tow results show that the calcification zone of *G. ruber* always extends down to the deep chlorophyll maximum. Therefore, in the water column structure where SML and DCM are separated by a seasonal thermocline, such as in summer at the CWR, the export $\delta^{18}\text{O}_c$ of *G. ruber* can underestimate the SST by more than 2°C .

[52] **Acknowledgments.** We thank the captains and crews of R/V *Pelagia* and R/V *Agulhas* as well as the NIOZ shipboard scientific parties for their assistance during the MARE cruises. G. C. Feldman and N. Kuring from the SeaWiFS provided the satellite derived chlorophyll *a* records. B. Hönisch (AWI–Bremerhaven) analyzed the $\delta^{18}\text{O}_w$ samples at the UC-Davis, by courtesy of H. Spero. Reviews by J. Bijma, S. Mulitza, and L. Peterson helped to improve the manuscript. This study was supported by the Netherlands-Bremen Oceanography (NEBROC) and the Mixing of *Agulhas* Rings Experiment (MARE) programs of the NWO/DFG and the NWO-ALW.

References

- Bemis, B. E., H. J. Spero, J. Bijma, and D. W. Lea (1998), Reevaluation of oxygen isotopic composition of planktonic foraminifera: Experimental results and revised paleotemperature equations, *Paleoceanography*, 13(2), 150–160.
- Bemis, B. E., H. J. Spero, D. W. Lea, and J. Bijma (2000), Temperature influence on the carbon isotopic composition of *Globigerina bulloides* and *Orbulina universa* (planktonic foraminifera), *Mar. Micropaleontology*, 38(3–4), 213–228.

- Berger, W. H., and A. Soutar (1967), Planktonic foraminifera: Field experiment on production rate, *Science*, 156, 1495–1497.
- Bijma, J., and C. Hemleben (1994), Population dynamics of the planktic foraminifer *Globigerinoides sacculifer* (Brady) from the central Red Sea, *Deep Sea Res., Part I*, 41(3), 485–510.
- Bijma, J., J. Erez, and C. Hemleben (1990), Lunar and semi-lunar reproductive cycles in some spinose planktonic foraminifers, *J. Foraminiferal Res.*, 20(2), 117–127.
- Bijma, J., C. Hemleben, and K. Wellnitz (1994), Lunar-influenced carbonate flux of the planktic foraminifer *Globigerinoides sacculifer* (Brady) from the central Red Sea, *Deep Sea Res., Part I*, 41(3), 511–530.
- Bijma, J., H. J. Spero, and D. W. Lea (1999), Reassessing foraminiferal stable isotope geochemistry: Impact of the oceanic carbonate system (experimental results), in *Use of Proxies in Paleoceanography: Examples From the South Atlantic*, edited by G. Fischer and G. Wefer, pp. 489–512, Springer, New York.
- Brummer, G.-J. A., C. Hemleben, and M. Spindler (1987), Ontogeny of extant spinose planktonic foraminifera (Globigerinidae): A concept exemplified by *Globigerinoides sacculifer* (Brady) and *G. ruber* (d'Orbigny), *Mar. Micropaleontol.*, 12(4), 17–49.
- Craig, H. (1965), The measurement of oxygen isotopes paleotemperatures, in *Spoleto Conference on Stable Isotopes in Oceanographic Studies and Paleotemperatures*, edited by E. Tongiorgi, pp. 3–24, Lab. Geol. Nucl., CNR, Pisa, Italy.
- Craig, H., and L. I. Gordon (1965), Isotopic oceanography: Deuterium and oxygen 18 variations in the ocean and the marine atmosphere, in *Marine Geochemistry*, edited by D. R. Schink and J. T. Corless, pp. 277–374, Univ. of R. I., Kingston.
- Darling, K. F., D. Kroon, C. M. Wade, and A. J. L. Brown (1996), Molecular phylogeny of the planktic foraminifera, *J. Foraminiferal Res.*, 26(4), 324–330.
- Darling, K. F., C. M. Wade, D. Kroon, and A. J. L. Brown (1999), The diversity and distribution of modern planktic foraminiferal small subunit ribosomal RNA genotypes and their potential as tracers of present and past ocean circulations, *Paleoceanography*, 14(1), 3–12.
- Deuser, W. G. (1987), Seasonal variations in isotopic composition and deep-water fluxes of the tests of perennially abundant planktonic foraminifera of the Sargasso Sea: Results from sediment trap collections and their paleoceanographic significance, *J. Foraminiferal Res.*, 17(1), 14–27.
- Deuser, W. G., and E. H. Ross (1989), Seasonally abundant planktonic foraminifera of the Sargasso Sea: Succession, deep-water fluxes, isotopic compositions, and paleoceanographic implications, *J. Foraminiferal Res.*, 19(4), 268–293.
- Deuser, W. G., E. H. Ross, C. Hemleben, and M. Spindler (1981), Seasonal changes in species composition, numbers, mass, size and isotopic composition of planktonic foraminifera settling into the deep Sargasso Sea, *Palaeogeogr. Palaeoclimatol. Palaeoecol.*, 33(1–3), 103–127.
- Duplessy, J. C., A. W. H. Bé, and P. L. Blanc (1981), Oxygen and carbon isotopic composition and biogeographic distribution of planktonic foraminifera in the Indian Ocean, *Palaeogeogr. Palaeoclimatol. Palaeoecol.*, 33(1–3), 9–46.
- Duplessy, J. C., L. Labeyrie, M. Arnold, M. Pateme, J. Duprat, and T. C. E. van Weering (1992), Changes in surface salinity of the North Atlantic Ocean during the last deglaciation, *Nature*, 358, 485–488.
- Epstein, S., R. Buchsbaum, H. A. Lowenstam, and H. C. Urey (1953), Revised carbonate-water isotopic temperature scale, *Geol. Soc. Am. Bull.*, 64, 1315–1326.
- Erez, J., and S. Honjo (1981), Comparison of isotopic composition of planktonic foraminifera in plankton tows, sediment traps and sediments, *Palaeogeogr. Palaeoclimatol. Palaeoecol.*, 33(1–3), 129–156.
- Erez, J., and B. Luz (1983), Experimental paleotemperature equation for planktonic foraminifera, *Geochim. Cosmochim. Acta*, 47(6), 1025–1031.
- Erez, J., A. Almogi-Labin, and S. Avraham (1991), On the life history of planktonic foraminifera: Lunar reproduction cycle in *Globigerinoides sacculifer* (Brady), *Paleoceanography*, 6(3), 295–306.
- Fairbanks, R. G., and P. H. Wiebe (1980), Foraminifera and chlorophyll maximum: Vertical distribution, seasonal succession and paleoceanographic significance, *Science*, 209(4464), 1524–1526.
- Fairbanks, R. G., P. H. Wiebe, and A. W. H. Bé (1980), Vertical distribution and isotopic composition of living planktonic foraminifera in the western North Atlantic, *Science*, 207(4426), 61–63.
- Fairbanks, R. G., M. S. Sverdrlove, R. Free, P. H. Wiebe, and A. W. H. Bé (1982), Vertical distribution and isotopic fractionation of living planktonic foraminifera from Panama Basin, *Nature*, 298, 841–844.
- Field, D. B. (2004), Variability in vertical distributions of planktonic foraminifera in the California Current: Relationships to vertical ocean structure, *Paleoceanography*, 19, PA2014, doi:10.1029/2003PA000970.
- Garzoli, S. L., and A. L. Gordon (1996), Origins and variability of the Benguela Current, *J. Geophys. Res.*, 101(C1), 897–906.
- Griffiths, F. B., G. H. Brown, D. D. Reid, and R. R. Parker (1984), Estimation of sample zooplankton abundance from Folsom splitter subsamples, *J. Plankton Res.*, 6(5), 721–731.
- Hemleben, C., and J. Bijma (1994), Foraminiferal population dynamics and stable carbon isotopes, in *Carbon Cycling in the Glacial Ocean: Constraints on the Ocean's Role in Global Change*, edited by R. Zahn et al., pp. 145–166, Springer, New York.
- Hemleben, C., M. Spindler, and O. R. Anderson (1989), *Modern Planktonic Foraminifera*, 363 pp., Springer, New York.
- Herbland, A., and B. Voituriez (1979), Hydrological structure analysis for estimating the primary production in the tropical Atlantic Ocean, *J. Mar. Res.*, 37, 87–101.
- Huber, B. T., J. Bijma, and K. Darling (1997), Cryptic speciation in the living planktonic foraminifer *Globigerinella siphonifera* (d'Orbigny), *Paleobiology*, 23(1), 33–62.
- Hut, G. (1987), Stable isotope reference samples for geochemical and hydrological investigations, Consultants Group Meeting, report, 42 pp., Int. At. Energy Agency, Vienna, Austria.
- Kemle-von Mücke, S., and H. Oberhänsli (1999), The distribution of living planktic foraminifera in relation to southeast Atlantic oceanography, in *Use of Proxies in Paleoceanography: Examples From the South Atlantic*, edited by G. Fisher and G. Wefer, pp. 91–115, Springer, New York.
- Kim, S. T., and J. R. O'Neil (1997), Equilibrium and nonequilibrium oxygen isotope effects in synthetic calcites, *Geochim. Cosmochim. Acta*, 61(16), 3461–3475.
- Kroon, D. (1988), Planktonic foraminifera as tracers of ocean-climate history, Ph.D. thesis, pp. 335–346, Vrije Univ., Amsterdam.
- Kroon, D., and K. Darling (1995), Size and upwelling control of the stable-isotope composition of *Neogloboquadrina dutertrei* (D'Orbigny), *Globigerinoides ruber* (D'Orbigny) and *Globigerina bulloides* (D'Orbigny): Examples from the Panama Basin and Arabian Sea, *J. Foraminiferal Res.*, 25(1), 39–52.
- LeGrande, A. N., J. Lynch-Stieglitz, and M. C. Farmer (2004), Oxygen isotopic composition of *Globorotalia truncatulinoides* as a proxy for intermediate depth density, *Paleoceanography*, 19(4), PA4025, doi:10.1029/2004PA001045.
- Levitus, S., and T. Boyer (1994), *World Ocean Atlas 1994*, vol. 4, 117 pp., U.S. Dep. of Commerce, Washington, D. C.
- Lohmann, G. P. (1992), Increasing seasonal upwelling in the subtropical South Atlantic over the past 700,000 yrs: Evidence from deep-living planktonic foraminifera, *Mar. Micropaleontol.*, 19(1–2), 1–12.
- Lohmann, G. P. (1995), A model for variation in the chemistry of planktonic foraminifera due to secondary calcification and selective dissolution, *Paleoceanography*, 10(3), 445–457.
- Lohmann, G. P., and P. N. Schweitzer (1990), *Globorotalia truncatulinoides*' growth and chemistry as probes of the past thermocline: 1. Shell size, *Paleoceanography*, 5(1), 55–75.
- Lončarić, N. (2005), Planktic foraminiferal response to changing SE Atlantic oceanography, Ph.D. thesis, 184 pp., Vrije Univ., Amsterdam, 15 Dec.
- Lončarić, N., G.-J. A. Brummer, and D. Kroon (2005), Lunar cycles and seasonal variations in deposition fluxes of planktic foraminiferal shell carbonate to the deep South Atlantic (central Walvis Ridge), *Deep Sea Res., Part I*, 52(7), 1178–1188.
- Lutjeharms, J. R. E. (1996), The exchange of water between the South Indian and South Atlantic oceans, in *The South Atlantic: Present and Past Circulation*, edited by G. Wefer et al., pp. 125–162, Springer, New York.
- Lutjeharms, J. R. E., and P. L. Stockton (1987), Kinematics of southern Africa's upwelling front, in *The Benguela and Comparable Ecosystems*, edited by A. I. L. Payne, J. A. Gulland and K. H. Brink, pp. 35–49, Sea Fish. Res. Inst., Cape Town.
- Mann, K. H., and J. R. N. Lazier (1991), *Dynamics of Marine Ecosystems*, 466 pp., Blackwell Sci., Malden, Mass.
- Mulitza, S., A. Dürkoop, W. Hale, G. Wefer, and H.-S. Niebler (1997), Planktonic foraminifera as recorders of past surface-water stratification, *Geology*, 25(4), 335–338.
- Mulitza, S., D. Boltovskoy, B. Donner, H. Meggers, A. Paul, and G. Wefer (2003a), Temperature: $\delta^{18}\text{O}$ relationships of planktonic foraminifera collected from surface waters, *Palaeogeogr. Palaeoclimatol. Palaeoecol.*, 202, 143–152.
- Mulitza, S., B. Donner, G. Fischer, A. Paul, J. Pätzold, C. Rühlemann, and M. Segl (2003b), The South Atlantic oxygen isotope record of planktic foraminifera, in *The South Atlantic in the Late Quaternary: Reconstruction of Material Budgets and Current Systems*, edited by G. Wefer, S. Mulitza and V. Ratmeyer, pp. 121–142, Springer, New York.
- Niebler, H.-S., H.-W. Hubberten, and R. Gersonde (1999), Oxygen isotope values of planktic for-

- aminifera: A tool for the reconstruction of surface water stratification, in *Use of Proxies in Paleoceanography: Examples From the South Atlantic*, edited by G. Fischer and G. Wefer, pp. 165–189, Springer, New York.
- Oberhänsli, H., C. Bénier, G. Meinecke, H. Schmidt, R. Schneider, and G. Wefer (1992), Planktonic foraminifera as tracers of ocean currents in the eastern South Atlantic, *Paleoceanography*, 7(5), 607–632.
- Ortiz, J. D., A. C. Mix, and R. W. Collier (1995), Environmental control of living symbiotic and asymbiotic foraminifera of the California Current, *Paleoceanography*, 10(6), 987–1009.
- Ortiz, J. D., A. C. Mix, W. Rugh, J. M. Watkins, and R. W. Collier (1996), Deep-dwelling planktonic foraminifera of the northeastern Pacific Ocean reveal environmental control of oxygen and carbon isotopic disequilibrium, *Geochim. Cosmochim. Acta*, 60(22), 4509–4523.
- Peeters, F. J. C. and G.-J. A. Brummer (2002), The seasonal and vertical distribution of living planktic foraminifera in the NW Arabian Sea, in *The Tectonic and Climatic Evolution of the Arabian Sea Region*, edited by P. D. Clift et al., *Geol. Soc. Spec. Publ.*, 195, 463–497.
- Peeters, F. J. C., G.-J. A. Brummer, and G. Ganssen (2002), The effect of upwelling on the distribution and stable isotope composition of *Globigerina bulloides* and *Globigerinoides ruber* (planktic foraminifera) in modern surface waters of the NW Arabian Sea, *Global Planet. Change*, 34(3–4), 269–291.
- Peterson, R. G., and L. Stramma (1991), Upper-level circulation in the South Atlantic Ocean, *Progr. Oceanogr.*, 26(1), 1–73.
- Ravelo, A. C., and R. G. Fairbanks (1992), Oxygen isotopic composition of multiple species of planktonic foraminifera: Recorders of the modern photic zone temperature gradient, *Paleoceanography*, 7(6), 815–831.
- Russell, A. D., and H. J. Spero (2000), Field examination of the oceanic carbonate ion effect on stable isotopes in planktonic foraminifera, *Paleoceanography*, 15(1), 43–52.
- Schiebel, R., and C. Hemleben (2000), Interannual variability of planktic foraminiferal populations and test flux in the eastern North Atlantic Ocean (JGOFS), *Deep Sea Res., Part II*, 47(9–11), 1809–1852.
- Schouten, M. W., W. P. M. de Ruijter, and P. J. van Leeuwen (2002), Upstream control of Agulhas Ring shedding, *J. Geophys. Res.*, 107(C8), 3109, doi:10.1029/2001JC000804.
- Schweitzer, P., and G. P. Lohmann (1991), Ontogeny and habitat of modern menardiiform planktonic foraminifera, *J. Foraminiferal Res.*, 21(4), 332–346.
- Sell, D. W., and M. S. Evans (1982), A statistical analysis of subsampling and an evaluation of Folsom plankton splitter, *Hydrobiologia*, 94(3), 223–230.
- Shackleton, N. J. (1974), Attainment of isotopic equilibrium between ocean water and the benthonic foraminifera genus *Uvigerina*: Isotopic changes in the last glacial, *Colloq. Int. C.N.R.S.*, 219, 203–209.
- Shackleton, N. J., and N. D. Opdyke (1973), Oxygen isotope and paleomagnetic stratigraphy of equatorial Pacific core V28–238: Oxygen isotope temperatures and ice volumes on a 10^5 and 10^6 year scale, *Quat. Res.*, 3, 39–55.
- Shannon, L. V., and G. Nelson (1996), The Benguela: Large scale features and processes and system variability, in *The South Atlantic: Present and Past Circulation*, edited by G. Wefer et al., pp. 163–210, Springer, New York.
- Simstich, J., M. Sarnthein, and H. Erlenkeuser (2003), Paired $\delta^{18}\text{O}$ signals of *Neogloboquadrina pachyderma* (s) and *Turborotalita quinqueloba* show thermal stratification structure in Nordic seas, *Mar. Micropaleontol.*, 48(1–2), 107–125.
- Spero, H. J., and D. W. Lea (1993), Intraspecific stable isotope variability in the planktic foraminifera *Globigerinoides sacculifer*: Results from laboratory experiments, *Mar. Micropaleontol.*, 22(3), 221–234.
- Spero, H. J., and D. F. Williams (1988), Extracting environmental information from planktonic foraminiferal $\delta^{13}\text{C}$ data, *Nature*, 335, 717–719.
- Spero, H. J., J. Bijma, D. W. Lea, and B. E. Bemis (1997), Effect of seawater carbonate ion concentration on foraminiferal carbon and oxygen isotopes, *Nature*, 390, 497–500.
- Thunell, R., and L. R. Sautter (1992), Planktonic foraminiferal fauna and stable isotopic indices of upwelling: A sediment trap study in the San Pedro Basin, Southern California Bight, in *Upwelling Systems: Evolution Since the Early Miocene*, edited by C. P. Summerhayes, W. L. Prell and K. C. Emeis, *Geol. Soc. Spec. Publ.*, 64, 77–91.
- Veth, C. (2000), RV *Pelagia* cruise report: Cruise 64PE155, Project MARE-1, Mixing of Agulhas Rings Experiment, NIOZ cruise reports, 42 pp. R. Neth. Inst. for Sea Res., Texel.
- Wiebe, P. H., and M. C. Benfield (2003), From the Hensen net toward four-dimensional biological oceanography, *Progr. Oceanogr.*, 56, 7–136.
- Williams, D. F., A. W. Bé, and R. G. Fairbanks (1981), Seasonal stable isotopic variations in living planktonic foraminifera from Bermuda plankton tows, *Palaeogeogr. Palaeoclimatol. Palaeoecol.*, 33(1–3), 71–102.
- Wolf-Gladrow, D. A., J. Bijma, and R. E. Zeebe (1999), Model simulation of the carbonate chemistry in the microenvironment of symbiont bearing foraminifera, *Mar. Chem.*, 64(3), 181–198.
- Zeebe, R. E. (1999), An explanation of the effect of the seawater carbonate concentration on foraminiferal oxygen isotopes, *Geochim. Cosmochim. Acta*, 63(13–14), 2001–2007.

G.-J. A. Brummer and N. Lončarić, Department of Marine Chemistry and Geology, NIOZ, P.O. Box 59, NL-1790 AB Den Burg, Texel, Netherlands. (neven.loncaric@zg.t-com.hr)

D. Kroon, Department of Geology and Geophysics, University of Edinburgh, Grant Institute, West Mains Road, Edinburgh EH9 3JW, UK.

F. J. C. Peeters, Department of Paleocology and Paleoclimatology, Faculty of Life and Earth Sciences, Vrije Universiteit Amsterdam, De Boelelaan 1085, NL-1081 HV Amsterdam, Netherlands.